

**Structure-function studies of the catalase-peroxidase BpKatG from**

***Burkholderia pseudomallei***

**by**

**Taweewat Deemagarn**

A thesis

Submitted to the Faculty of Graduate Studies

In partial fulfillment of the requirements for the degree of

**MASTER OF SCIENCE**

Department of Microbiology

University of Manitoba

Winnipeg, Manitoba

Canada

© Taweewat Deemagarn, July 2004

**THE UNIVERSITY OF MANITOBA**  
**FACULTY OF GRADUATE STUDIES**  
\*\*\*\*\*  
**COPYRIGHT PERMISSION**

**Structure-function studies of the catalase-peroxidase BpKatG from**  
*Burkholderia pseudomallei*

**BY**

**Taweewat Deemagarn**

**A Thesis/Practicum submitted to the Faculty of Graduate Studies of The University of**  
**Manitoba in partial fulfillment of the requirement of the degree**  
**Of**  
**MASTER OF SCIENCE**

**Taweewat Deemagarn © 2004**

**Permission has been granted to the Library of the University of Manitoba to lend or sell copies of this thesis/practicum, to the National Library of Canada to microfilm this thesis and to lend or sell copies of the film, and to University Microfilms Inc. to publish an abstract of this thesis/practicum.**

**This reproduction or copy of this thesis has been made available by authority of the copyright owner solely for the purpose of private study and research, and may only be reproduced and copied as permitted by copyright laws or with express written authorization from the copyright owner.**

## ABSTRACT

*Burkholderia pseudomallei* produces catalase-peroxidase (BpKatG) encoded by the *katG* gene as part of its cellular defence system against oxidative stress either as catalase or as peroxidase. BpKatG is 65% identical with KatG of *Mycobacterium tuberculosis*, the enzyme responsible for the activation of isoniazid, the anti-tubercular drug. A structure-function study of BpKatG was carried out via site-directed mutagenesis, focusing mainly on residues on the distal side of the heme active site. Changing the Arg108, His112 and Asp141 residues in BpKatG resulted in significant changes in enzymatic activities as well as changes in absorption spectra and susceptibility to inhibitors. Changes to His112 caused drastically decreased catalase and peroxidase activities, while changes to Arg108 lowered catalase and peroxidase activities, but not as much as changes to His112. These data have confirmed a catalytic role for His112 and Arg108 in compound I formation. Changes to Asp141 caused significantly decreased catalase activity when Ala and Asn were the replacing residues but not when Glu was the replacement. None of the replacements affected peroxidase activity. This result confirmed that Asp141 is involved in compound I reduction by H<sub>2</sub>O<sub>2</sub>, but not in compound I formation. Two mechanisms are presented to explain the involvement of Asp141 in compound I reduction, direct ionic interaction with the substrate and a possible electrical potential field effect.

## ACKNOWLEDGEMENTS

I would like to express my great appreciation to my advisor, Dr. Peter Loewen for his expertise, guidance, patience and continuous support during my study. I would also like to thank members of my advisory committee, Dr. Barbara Triggs-Raine, Dr. Michael Mulvey and Dr. Teresa De Kievit for their useful suggestions and encouragement throughout the progression of this research. I am also thankful to Mr. Jacek Switala for his invaluable technical assistance. My thanks are extended to all faculty members and support staff in the Department of Microbiology for their kindness and assistance. Thanks also go to the Loewen lab members, Ben, Rahul, Inderpal, Sherif, Prashen, Ajith, Xavi, Sukheon, and Jocylyn and to graduate students in Department of Microbiology for their friendship. Financial support from the Royal Thai Government was greatly appreciated. Last, but certainly not least, I wish to give my special thanks to my parents, my wife and my daughters for their love, encouragement, support and understanding.

## TABLE OF CONTENTS

	Page
<b>ABSTRACT.....</b>	ii
<b>ACKNOWLEDGEMENTS.....</b>	iii
<b>TABLE OF CONTENTS.....</b>	iv
<b>LIST OF FIGURES.....</b>	vii
<b>LIST OF TABLES.....</b>	viii
<b>LIST OF ABBREVIATIONS.....</b>	ix
 <b>1. GENERAL INTRODUCTION.....</b>	 1
1.1. The paradox of oxygen.....	1
1.1.1. Oxygen toxicity.....	2
1.1.2. Detoxification systems: Antioxidant defences.....	3
1.2. Catalases.....	4
1.2.1. Introduction.....	4
1.2.2. Categorization.....	5
1.2.2.1. Monofunctional catalases.....	5
1.2.2.2. Bifunctional catalase-peroxidases.....	6
1.2.2.3. Non-heme catalases.....	6
1.2.2.4. Minor catalases.....	6
1.3. Monofunctional catalases.....	7
1.3.1. Mechanism.....	7
1.3.2. Catalase structure.....	8
1.3.3. An electrical potential field in the channel of monofunctional catalases.....	9
1.4. Catalase-Peroxidases.....	10
1.4.1. Structure and function.....	10
1.4.2. The role of KatG in INH activation.....	12

1.5. Catalase-peroxidase of <i>Burkholderia pseudomallei</i> (BpKatG).....	14
1.5.1. The unusual covalent modifications.....	15
1.5.1.a. A covalent adduct structure linked Trp111-Try238-Met264.....	16
1.5.1.b. Heme modification.....	17
1.5.2. Substrate access channels.....	17
1.6. Objectives of thesis.....	19
 2. MATERIALS AND METHODS.....	 21
2.1. <i>Escherichia coli</i> strains, plasmids and bacteriophage.....	21
2.2. Biochemicals and common reagents.....	21
2.3. Media, growth conditions and storage of stock cultures.....	24
2.4. DNA manipulation.....	25
2.4.1. Preparation of synthetic oligonucleotides.....	25
2.4.2a. Site-directed mutagenesis strategy.....	25
2.4.2b. Reconstruction of <i>B. pseudomallei</i> <i>katG</i> subclones with desired mutation.....	27
2.4.3. DNA isolation and purification.....	27
2.4.4. Restriction endonuclease digestion of DNA.....	36
2.4.5. Agarose gel electrophoresis.....	36
2.4.6. Ligation.....	36
2.4.7. Transformation.....	37
2.4.8. DNA sequencing.....	37
2.5. Purification of BpKatG and its variants.....	38
2.6. Sodium dodecyl sulfate-polyacrylamide gel electrophoresis (SDS-PAGE).....	41
2.7. Enzymatic assays and protein quantitation.....	41
2.8. Absorption spectrophotometry.....	44
2.9. Effects of inhibitors.....	45

<b>3. RESULTS.....</b>	<b>46</b>
3.1. Introduction.....	46
3.2. Characterization of BpKatG and its variants.....	46
3.3. Biochemical characterization of BpKatG and its variants.....	55
3.4. Kinetic characterization.....	54
3.5. Effect of heme inhibitors on the catalase activity.....	58
<b>4. DISCUSSION.....</b>	<b>73</b>
4.1. Structure-function studies on BpKatG.....	73
4.2. Future directions.....	76
<b>5. REFERENCES.....</b>	<b>78</b>

## LIST OF FIGURES

Figure	Page
1.1. Amino acid sequence of catalase-peroxidase BpKatG.....	20
2.1. Simplified restriction map of the chromosomal inserts containing the <i>B. pseudomallei katG</i> gene in plasmids pBpG, pBpG-KH and pBpG-KC.....	23
2.2. General reconstruction protocol used for generation of variant <i>katG</i> 's from mutagenized subclone I for protein expression.....	29
2.3. Nucleotide sequence of <i>Burkholderia pseudomallei katG</i> showing the restriction sites, the sequencing primers (BpG 1-6) and mutagenic oligonucleotides indicating base changes.....	30
3.1. Two views of residues in the active site of BpKatG related by a 90° rotation...	48
3.2. SDS-polyacrylamide gel electrophoretic analysis of purified BpKatG and its variants.....	50
3.3. Absorption spectra of wild type BpKatG and its variants.....	51
3.4. Effect of H <sub>2</sub> O <sub>2</sub> concentration on the initial catalatic velocities (V <sub>i</sub> ) of wild type BpKatG and its variants.....	60
3.5. Effect of ABTS concentration on the initial peroxidatic velocities (V <sub>i</sub> ) of wild type BpKatG and its variants.....	65
3.6. Comparison of the effect of potassium cyanide (KCN) on the catalase activity of wild type BpKatG and its variants.....	70
3.7. Comparison of the effect of sodium azide (NaN <sub>3</sub> ) on the catalase activity of wild type BpKatG and its variants.....	71
4.1. Hypothetical scheme for the mechanism of Compound I formation and reduction during the catalatic turnover of catalase-peroxidase.....	77



## LIST OF TABLES

Table	Page
2.1. List of <i>Escherichia coli</i> strains, plasmids and bacteriophage used in this study.....	22
2.2. Sequences of oligonucleotides used for site-directed mutagenesis of <i>BpkatG</i> ...	28
3.1. Purification of wild type BpKatG from the <i>Escherichia coli</i> strain UM262 harbouring plasmid encoded <i>katG</i> of <i>Burkholderia pseudomallei</i> .....	49
3.2. Summary of observed optical absorbance maxima, $A_{407/280}$ and heme/subunit ratios for purified of BpKatG and its variants.....	54
3.3. Catalase and peroxidase activities of BpKatG and its variants.....	56
3.4. NADH oxidase and INH hydrazinolysis activities of BpKatG and its variants.	57
3.5. Comparison of the observed catalatic kinetic parameters of purified wildtype BpKatG and its variants, using $H_2O_2$ as substrate.....	64
3.6. Comparison of the observed peroxidatic kinetic parameters of purified wildtype BpKatG and its variants, using ABTS as substrate.....	69
3.7. Comparison of sensitivity of BpKatG and its variants to cyanide (KCN) and azide ( $NaN_3$ ).....	72

## LIST OF ABBREVIATIONS

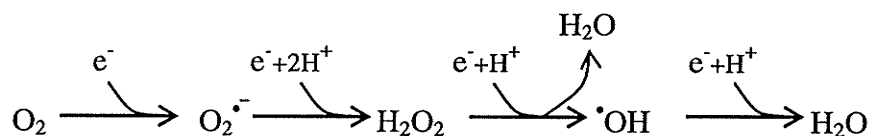
A	Absorbance
ABTS	2,2'-azinobis(3-ethylbenzothiazolinesulfonic acid)
Amp <sup>R</sup>	Ampicillin resistant
APX	Ascorbate peroxidase
BLC	Bovine liver catalase
bp	Base pair(s)
BpKatG	Catalase-peroxidase from <i>Burkholderia pseudomallei</i>
CCP	Cytochrome c peroxidase
Ci	Curie
CIP	Calf intestinal alkaline phosphatase
Da	Dalton(s)
DEAE	Diethylaminoethyl
DMSO	Dimethylsulfoxide
DNA	Deoxyribonucleic acid
dNTP	Deoxyribonucleoside triphosphate
e <sup>-</sup>	Electron
EcKatG	Catalase-peroxidase from <i>Escherichia coli</i>
EDTA	Ethylenediaminetetraacetic acid
H <sup>+</sup>	Proton
HmCPx	Catalase-peroxidase from <i>Haloarcula marismortui</i>
H <sub>2</sub> O	Water
H <sub>2</sub> O <sub>2</sub>	Hydrogen peroxide
HPI	Hydroperoxidase I
HPII	Hydroperoxidase II
HRP	Horseradish peroxidase
INH	Isonicotinic acid hydrazide (isoniazid)
Kbp	Kilo base pair(s)
k <sub>cat</sub>	Turnover number
kDa	KiloDalton(s)
K <sub>m</sub>	Michealis-Menten constant

LB	Luria-Bertani
$\mu\text{M}$	Micromolar
M	Molarity/molar
mg	Milligram(s)
ml	Millilitre
mM	Millimolar
MtKatG	Catalase-peroxidase from <i>Mycobacterium tuberculosis</i>
NADH	Nicotinamide adenine dinucleotide
NADPH	Nicotinamide adenine dinucleotide phosphate
NBT	Nitroblue tetrazolium
nm	Nanometer(s)
$\text{O}_2^{\bullet -}$	Superoxide anion radical
OD	Optical density
$\cdot\text{OH}$	Hydroxyl radical
ORF	Open reading frame
PAGE	Polyacrylamide gel electrophoresis
RNA	Ribonucleic acid
RNase	Ribonuclease
ROS	Reactive oxygen species
SDS	Sodium dodecyl sulfate
SOD	Superoxide dismutase
SyKatG	Catalase-peroxidase from <i>Synechococcus</i>
TE buffer	Tris-EDTA buffer
Tris	Tris (hydroxymethyl) aminomethane
U	Unit
V	Volts
$V_i$	Initial velocity
$V_{\text{max}}$	Maximum velocity
v/v	Volume per unit volume
w/v	Weight per unit volume

## 1. GENERAL INTRODUCTION

### 1.1. The paradox of oxygen

The fact that aerobic organisms need oxygen to survive and yet must constantly protect themselves against oxygen toxicity is frequently referred to as the oxygen paradox (Ho *et al.*, 1995). Although oxygen is essential to aerobic organisms as a final electron acceptor, it is toxic to these organisms as well because of partially reduced forms of oxygen formed during normal aerobic metabolism. Partially reduced forms of oxygen, including superoxide anion radical ( $O_2^{\bullet -}$ ), hydrogen peroxide ( $H_2O_2$ ) and hydroxyl radical ( $\bullet OH$ ), are generally termed reactive oxygen species (ROS). They are formed by the sequential univalent reduction of oxygen to water shown schematically below (modified from Fridovich, 1978):



The paramagnetism of oxygen in the ground state indicates that it contains two unpaired electrons of parallel spin in separate  $\pi^*$  antibonding orbitals. This can be illustrated as molecular-orbital diagram as follows (modified from Imlay, 2003):

$\sigma_x^*$			
$\pi_y^*, \pi_x^*$	$\underline{\uparrow} \quad \underline{\uparrow}$	$\underline{\uparrow\downarrow} \quad \underline{\uparrow}$	$\underline{\uparrow\downarrow} \quad \underline{\uparrow\downarrow}$
$\pi_y, \pi_x$	$\underline{\uparrow\downarrow} \quad \underline{\uparrow\downarrow}$	$\underline{\uparrow\downarrow} \quad \underline{\uparrow\downarrow}$	$\underline{\uparrow\downarrow} \quad \underline{\uparrow\downarrow}$
$\sigma_x$	$\underline{\uparrow\downarrow}$	$\underline{\uparrow\downarrow}$	$\underline{\uparrow\downarrow}$
	$O_2$	$O_2^{\bullet -}$	$H_2O_2$

This electronic structure constitutes a barrier to the oxygen reduction by an electron pair of antiparallel spin. Therefore, the electrons are preferentially transferred to oxygen one at a time by a sequential univalent pathway (Fridovich, 1999). When molecular oxygen is reduced by one electron, the electron must enter one of the  $\pi^*$  antibonding orbitals. The product is superoxide radical ( $O_2^{\bullet-}$ ) with only one unpaired electron as shown in the diagram above. The addition of a second electron and two protons to  $O_2^{\bullet-}$  at physiological pH gives rise to hydrogen peroxide ( $H_2O_2$ ), an oxidizing species that has no unpaired electrons and, therefore, is not a free radical. The one electron reduction of  $H_2O_2$  with one proton yields  $H_2O$  and hydroxyl radical ( $\bullet OH$ ), the strongest oxidant produced in biological systems. Generation of  $\bullet OH$  from  $H_2O_2$  is catalyzed by transition metals, particularly iron and copper. Finally,  $\bullet OH$  reduction produces a second molecule of  $H_2O$ . Together,  $O_2^{\bullet-}$ ,  $H_2O_2$  and  $\bullet OH$  are known as reactive oxygen species (ROS) and are continuously produced by aerobically growing cells (Castro and Freeman, 2001).

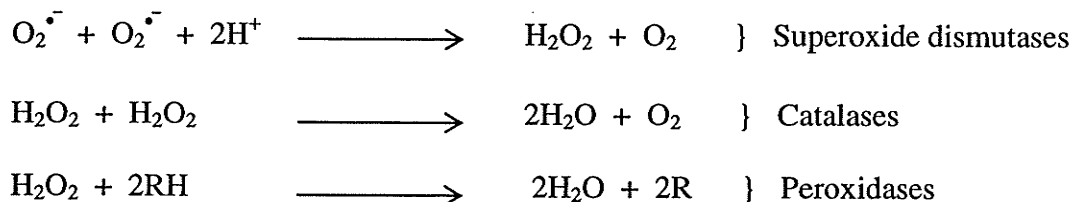
#### 1.1.1. Oxygen toxicity

$O_2^{\bullet-}$  and  $H_2O_2$  are unavoidable by-products of aerobic metabolism, because they are formed whenever molecular oxygen chemically oxidizes electron carriers such as flavoproteins (Storz and Imlay, 1999). Studies in *Escherichia coli* determined that autoxidations of NADH dehydrogenase II, succinate dehydrogenase, sulfite reductase, and fumarate reductase each generated  $O_2^{\bullet-}$  and  $H_2O_2$  when the reduced enzymes were exposed to oxygen. These ROS can also be derived from external environment factors such as the redox active drug (paraquat), radiation (ultraviolet rays), and heavy metals (Cabiscol *et al.*, 2000b). In addition, some immune cells, which use NADPH oxidase,

upon invasion by pathogenic bacteria, also exploit ROS as a weapon during phagocytosis (Cabiscol *et al.*, 2000a). In aerobic environments, mutant organisms that cannot scavenge endogenous  $O_2^{\cdot-}$  and  $H_2O_2$  typically grow poorly or die, indicating that these species are formed in potentially toxic doses inside living cells (Messner and Imlay, 2002). ROS can cause extensive damage to biological molecules including lipids, protein, DNA and RNA (Cabiscol *et al.*, 2000a). ROS can also damage proteins by either oxidizing amino acids or modifying prosthetic groups or metal clusters. DNA is a critical target for oxidative damage and the DNA lesions caused by oxidants can disrupt replication and lead to mutations (Demple and Harrison, 1994). However, neither superoxide radical nor hydrogen peroxide are themselves strong enough oxidizing agents to damage DNA. Much of the damage to DNA is caused by the hydroxyl radical generated from  $H_2O_2$  via the Fenton reaction, which requires a divalent metal ion, such as iron or copper and a source of reducing equivalents (possibly NADH) to reduce the metal.

#### **1.1.2. Detoxification systems: Antioxidant defences**

Aerobic organisms have developed detoxification systems to protect themselves from oxygen toxicity. The primary mechanism involves superoxide dismutases, catalases, and peroxidases that catalytically scavenge the intermediates of oxygen reduction. The superoxide radical is eliminated by superoxide dismutases, which catalyze its conversion to hydrogen peroxide plus oxygen. The hydrogen peroxide, in turn, is removed by either catalases, which convert it to water plus oxygen, or by peroxidases, which reduce it to water, using a variety of reductants available in the cell. The reactions catalyzed by these enzymes are shown below (modified from Fridovich, 1978):



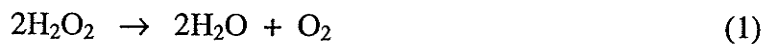
It is clear that efficient removal of the first two intermediates of oxygen reduction  $\text{O}_2^{\bullet-}$  and  $\text{H}_2\text{O}_2$ , will prevent formation of  $\cdot\text{OH}$ , the highly reactive hydroxyl radical (Fridovich, 1978).

In addition to the detoxification systems described above, several repair enzymes also constitute secondary mechanisms that serve to minimize the damage caused by toxic oxygen species. This group include methionine sulfoxide reductases to reverse the oxidation of methionine residue, proteases to hydrolyse oxidized proteins, endonucleases to remove oxidized bases from nucleic acids and begin the process of repair, and phospholipases to hydrolyse oxidized phospholipids (Fridovich, 1999).

## 1.2. Catalases

### 1.2.1. Introduction

Catalase, also called hydroperoxidase, is a protective enzyme. It was first biochemically characterized and named in 1900 (Loew, 1900). The overall reaction for catalases is the degradation of two molecules of hydrogen peroxide to water and oxygen (reaction 1) to prevent the formation of the more reactive hydroxyl radical.



This simple overall reaction can be broken down into two stages, the details of which differ depending on the type of catalase and will be described below. In order to protect themselves against reactive oxygen species by catalases, most aerobic organisms produce at least one catalase from among the three main classes of the enzyme (Loewen, 1999).

### **1.2.2. Categorization**

According to the diversity of structures and sequences and the different prosthetic groups, the proteins that exhibit significant catalase activity are classified into three groups: the monofunctional catalases, the bifunctional catalase-peroxidases and the non-heme catalases (Chelikani *et al.*, 2003)

#### **1.2.2.1. Monofunctional catalases**

The monofunctional catalases are the most widespread in nature and the most extensively characterized class. This class of heme-containing enzymes can be further subcategorized based on subunit size and the difference in heme prosthetic group. The first subclass is the small (<60 kDa) subunit catalase containing heme *b* such as bovine liver catalase. The small-subunit catalases have been found in prokaryotes, eukaryotes and a limited number of archael species. The second subclass is the large (>75 kDa) subunit catalase containing heme *d* such as hydroperoxidase II from *Escherichia coli*. The large-subunit catalases are restricted to fungi and bacteria (Loewen, 1999). This group will be discussed in detail in section 1.3.



#### 1.2.2.2. Bifunctional catalase-peroxidases

Catalase-peroxidases constitute the second largest class of catalases. They are bifunctional hemoproteins that exhibit a significant organic peroxidase activity in addition to the catalatic activity (Nicholls *et al.*, 2001). They have been characterized in both bacteria (Loewen, 1997) and fungi (Fraaije *et al.*, 1996; Levy *et al.*, 1992). This group will be discussed in detail in section 1.4.

#### 1.2.2.3. Non-heme catalases

The third and smallest class includes the non-heme or Mn-containing catalases. Currently there are only three non-heme catalases so far characterized, *Lactobacillus plantarum*, *Thermoleophilum album*, and *Thermus thermophilus*, but several more have been sequenced, all of bacteria origin. The active site of each of the three enzymes contains a manganese-rich reaction centre rather than a heme group (Kono and Fridovich, 1983; Allgood and Perry, 1986; Waldo *et al.*, 1991).

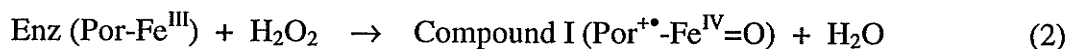
#### 1.2.2.4. Minor catalases

Additionally, a miscellaneous group of proteins, all heme-containing such as chloroperoxidase, plant peroxidase and myoglobin, exhibit very low levels of catalase activity, attributable to the presence of heme, which alone exhibits catalatic activity (Nichols *et al.*, 2001).

### 1.3. Monofunctional catalases

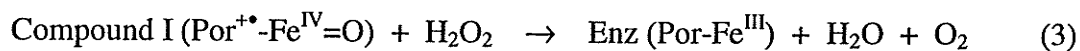
#### 1.3.1. Mechanism

All heme-containing monofunctional catalases have in common a two-stage mechanism for degradation of two molecules of  $\text{H}_2\text{O}_2$ . In the first stage, Compound I formation involves oxidation of the heme iron using one molecule of hydrogen peroxide as substrate. Compound I is an oxyferryl species with one oxidation equivalent located on the iron and a second oxidation equivalent delocalised in a heme cation radical (reaction 2).



Compound I is a short-lived catalytic intermediate with a distinct absorption spectrum characterized by a reduction in absorption intensity of the Sorêt band (at approximately 406 nm; a band which is diagnostic of hemoprotein). The formation of compound I is believed to be initiated by a histidine side-chain in the active site above the plane of the heme. The histidine acts as a general base donating electrons in a hydrogen bond with the hydrogen peroxide molecule coordinated to the heme iron. This facilitates formation of a transition complex, which is stabilized by additional hydrogen bond interactions with an asparagine. This allows scission of the peroxide O-O bond, to form compound I and one molecule of water (Fita and Rossman, 1985).

The second stage, or reduction of compound I, employs a second molecule of hydrogen peroxide as electron donor providing two reducing equivalents (reaction 3).



### 1.3.2. Catalase structure

Generally, the monofunctional catalases are active as tetramers, but dimers, hexamers, even an unusual heterotrimer structure (from *Pseudomonas aeruginosa*) have been reported, but not confirmed. To date, the crystal structures of nine monofunctional catalases have been determined, including the enzymes from bovine liver (BLC) (Murthy *et al.*, 1981; Fita *et al.*, 1986), *Penicillium vitale* (PVC) (Vainshtein *et al.*, 1981 and 1986), *Micrococcus lysodeikticus* (MLC) (Murshudov *et al.*, 1982), *Proteus mirabilis* (PMC) (Gouet *et al.*, 1995), *Escherichia coli* (HPH) (Bravo *et al.*, 1995 and 1999), *Saccharomyces cerevisiae* (CATA) (Berthet *et al.*, 1997; Maté *et al.*, 1999), human erythrocytes (HEC) (Ko *et al.*, 1999; Putnam *et al.*, 1999), *Pseudomonas syringae* (CatF) (Carpena *et al.*, 2001 and 2003), and *Helicobacter pylori* (HPC) (Loewen *et al.*, 2004). The typical features of a heme-containing catalase include an active site deeply buried in a beta-barrel core and two or three channels providing access to the heme (Loewen *et al.*, 2004). The recent reports of HPH variant structure (Chelikani *et al.*, 2003) and CatF (Carpena *et al.*, 2003) have provided significant insights into the channel architecture in catalases. Three obvious channels connect the heme-containing active site with the surface. The main channel is the most obvious access route to the heme. It approaches the heme perpendicular to its plane and has long been considered the primary access route for substrate  $H_2O_2$ . A second channel approaches the heme laterally, almost in the plane of the heme, and has been referred to as the minor or lateral channel. A third channel connects the heme with the central cavity, but no evidence of it having a role has been presented.

### 1.3.3. An electrical potential field in the channel of monofunctional catalases

A recent site-directed mutagenesis study of the conserved Asp (181 in HP11) demonstrated that replacement with any uncharged residue, polar or nonpolar, including Asn, Gln, Ala, Ser and Ile caused a loss of enzyme activity and a reduction in solvent occupancy in the channel (Chelikani *et al.*, 2003). Most notably, the sixth ligand water was absent in all subunits of D181A, D181S and D181Q variants, and there were generally fewer waters in the channel. By contrast, the D181E variant exhibited normal levels of activity and contained not only the sixth ligand water in all subunits, but an unbroken water matrix extending the full length of the channels. The striking influence of the negatively charged side chain at position 181 of HP11 may lie in the generation of an electrical potential field in the hydrophobic portion of the channel between the negative charge and the positive charged heme iron. The potential field will influence the orientation of any molecule with an electrical dipole, including both water and hydrogen peroxide. In both cases, the preferred orientation will be with oxygen atom pointed toward the positively charged heme iron and the hydrogens toward the negatively charged side chain of aspartate or glutamate. Such a uniform orientation in the population of solvent will facilitate the formation of hydrogen bonds, providing an explanation for increased water occupancy when Asp or Glu are present at position 181 in HP11. A second result of the induced orientation of hydrogen peroxide is that it will enter the active site with one oxygen oriented toward the heme iron, the hydrogen on this oxygen located within hydrogen bonding distance of the essential His and the second oxygen situated within hydrogen-bonding distance of the NH<sub>2</sub> of the active site Asn. This perfectly explains the suggestion arising from molecular dynamics studies that the

substrate hydrogen peroxide enters the active site in a preferred orientation (Chelikani *et al.*, 2003).

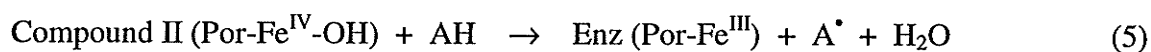
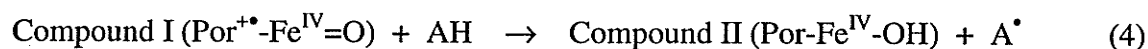
## **1.4. Catalase-peroxidases**

### **1.4.1. Structure and mechanism**

The bifunctional catalase-peroxidases are found in a wide variety of organisms including bacteria, archaeobacteria and fungi (Nicholls *et al.*, 2001). The first catalase-peroxidase HPI of *E.coli* was purified and characterized in 1979 (Claiborne and Fridovich, 1979), and the sequence of its encoding gene, *katG*, appeared in 1988 (Triggs-Raine *et al.*, 1988), providing the first catalase-peroxidase sequence demonstrating the sequence similarities to plant peroxidases.

The large size of the catalase-peroxidase subunit, which contains two distinct sequence-related domains, relative to the plant peroxidases may have been the result of a gene duplication and fusion event (Welinder, 1991). The N-terminal domain contains heme and active site residues that when modified affect enzyme activity. The C-terminal domain has less sequence similarity, does not seem to bind heme and does not have the well-conserved active site motif characteristic of peroxidases. For many years it was thought that heme occupancy for many catalase-peroxidases was partial, with an average of 0.5 heme per subunit in a heterogeneous mixture of dimers and tetramers with 0, 1 and 2 or 1, 2 and 3 hemes respectively (Hillar *et al.*, 2000). However, a more accurate determination of the molar extinction coefficient in light of the protein sequence has shown this to be incorrect.

Although the sequence and structure of catalase-peroxidases are different from the monofunctional catalases, their overall catalytic reaction takes place via the same two stages (reactions 2 and 3) as were described for the monofunctional catalases. This is because both types of enzyme contain heme and their active site residues seem to have similar roles albeit with arginine replacing asparagine. The main difference in the enzymatic mechanism between catalases and peroxidases is compound I reduction. The peroxidatic reaction presents another layer of complexity involving the uses of organic electron donors instead of  $\text{H}_2\text{O}_2$  for the reduction of compound I to the resting state via two one-electron transfers (reactions 4 and 5).



In the presence of a suitable organic electron donor and low levels of  $\text{H}_2\text{O}_2$ , the peroxidatic reaction becomes significant. Unfortunately, the *in vivo* peroxidatic substrate for the catalase-peroxidase has not been identified, leaving the actual role of the peroxidatic reaction undefined (Chelikani *et al.*, 2003).

The catalase-peroxidases were brought to researchers' attention around the world in 1992 when it was confirmed that a mutation of the *katG* gene encoding the *Mycobacterium tuberculosis* catalase-peroxidase causes resistance to isoniazid, an antitubercular pro-drug (Zhang *et al.*, 1992). This stimulated several groups worldwide to attempt to crystallize the protein in order to characterize at the molecular level the interaction of the protein with the drug. Unfortunately, attempts to crystallize a number of

different catalase-peroxidases were not successful until a decade later when the preliminary analyses of the crystallization of catalase-peroxidase from the halophilic archaeobacterium *Haloarcula marismortui* (Yamada *et al.*, 2001), from the cyanobacterium *Synechococcus* (Wada *et al.*, 2002), from the Gram-negative bacterium *Burkholderia pseudomallei* (Carpena *et al.*, 2002), and of the C-terminal domain of HPI of *E. coli* (Carpena *et al.*, 2002) were reported. The crystal structure of catalase-peroxidase from the *H. marismortui* enzyme (HmCPx) at 2.0 Å was reported first (Yamada *et al.*, 2002), followed by the structure of *B. pseudomallei* enzyme (BpKatG) at 1.7 Å (Carpena *et al.*, 2003). Both enzymes have similar structures with two subunits in the asymmetric unit, consistent with the predominant form of the enzyme in solution being a dimer. Each subunit is composed of 20- $\alpha$ -helical sections joined by linker regions and just three or four  $\beta$ -strand segments, making the structure very different from monofunctional catalases (Carpena *et al.*, 2003).

#### **1.4.2. The role of KatG in INH activation**

Tuberculosis is the world's leading cause of death from a single infectious agent. It is estimated that one-third of the world population is infected with *Mycobacterium tuberculosis*, with more than eight million new cases every year and almost two million deaths annually. The difficulty in controlling tuberculosis has increased by the worldwide rise of multidrug-resistant strains of *M. tuberculosis*, including resistance to isoniazid (INH), the most effective and widely used chemotherapeutic agent in treating the disease (Espinal and Raviglione, 2003). This has led to an urgent need for understanding the

molecular mechanism of drug resistance, in order to assist in the discovery and development of new drugs.

Isonicotinic acid hydrazide (isoniazid or INH) has been one of the first choice medications used in the treatment of tuberculosis since 1951, but the mode of action of this compound is still not completely understood (Madkour *et al.*, 2003). INH is considered as a *pro*-drug since its antituberculosis function requires activation by the catalase-peroxidase enzyme or KatG from *M. tuberculosis* (MtKatG)(Zhang *et al.*, 1992). This fact was reported shortly after the introduction of INH therapy when INH-resistant strains of *M. tuberculosis* were often accompanied by loss of catalase-peroxidase activity (Middlebrook, 1952 and 1954). This observation was confirmed by the molecular genetic studies of Zhang and colleagues who demonstrated that INH-sensitivity could be restored by introduction of the *katG* gene into an INH-resistant, catalase-deficient strain (Zhang *et al.*, 1992 and 1993). The elegant studies by this group have attracted worldwide attention. Numerous reports have subsequently demonstrated that mutation in, or deletion of, the *katG* gene results in the acquisition of isoniazid resistance (Heym *et al.*, 1995; Morris *et al.*, 1995; Rouse *et al.*, 1996; Saint-Joanis *et al.*, 1999). In parallel with the studies of INH-resistance correlating with a defect in the *katG* gene, the toxic effect of INH on *M. tuberculosis* has been studied showing that INH inhibits mycolic acid biosynthesis required for cell wall synthesis, leading to cell death (Winder and Collins, 1970; Takayama *et al.*, 1972 and 1975). However there is a controversy as to which enzymes of the mycolic acid pathway are the actual targets of INH (Kremer *et al.*, 2003). At least two enzymes have been identified as potential targets of activated INH, the enoyl-ACP reductase InhA (Banerjee *et al.*, 1994) and the  $\beta$ -ketoacyl-ACP synthase KsA (Mdluli *et*



*al.*, 1998). The X-ray crystallographic studies have revealed that InhA is probably the primary target of INH (Dessen *et al.*, 1995; Rozwarski *et al.*, 1998), revealing isonicotinoyl-NAD bound in the active site of InhA. This suggests that the active form of INH, probably an isonicotinoyl radical, reacts with  $\beta$ -nicotinamide adenine dinucleotide (NAD<sup>+</sup>/NADH), which is the cofactor of the long-chain enoyl-acyl carrier protein reductase InhA, a key enzyme in biosynthesis of long-chain fatty acids and of mycolic acid, specific components of the mycobacterial cell wall. The formation of isonicotinoyl-NAD, which acts as competitive inhibitors, explains the inactivation of InhA (Nguyen *et al.*, 2001). KatG significantly enhances the production of isonicotinoyl-NAD through the generation of isonicotinoyl radical, but it has not been convincingly demonstrated how the isonicotinoyl radical is combined with NADH and whether the KatG also facilitates this process (Chelikani *et al.*, 2003).

### 1.5. Catalase-peroxidase of *Burkholderia pseudomallei* (BpKatG)

*Burkholderia pseudomallei*, formerly called *Pseudomonas pseudomallei*, is a gram-negative rod bacterium that causes an acute and fatal septicaemia melioidosis in humans (Loprasert *et al.*, 2002). The disease is endemic in Southeast Asia, tropical countries and northern Australia and it is being increasingly recognized as a potential biological weapon (Leelarasamee, 2004). *B. pseudomallei* survives in phagocyte cells (Jones *et al.*, 1996) and as an intracellular pathogen, it has adopted various strategies to evade host defence mechanisms, including protection against reactive oxygen species produced by the phagocyte cells of the host (Miyagi *et al.*, 1997). Catalase-peroxidase of

*B. pseudomallei* (BpKatG) is one of the antioxidant enzymes that plays a significant protective role against such oxidative threats (Loprasert *et al.*, 2003). The sequence of the *katG* gene appeared in 2002 (Loprasert *et al.*, 2002), and the purification and crystallization of the enzyme appeared the same year. BpKatG shows high sequence similarity to other catalase-peroxidases of bacterial, archaeobacterial and fungal origin including 65% identity to KatG from *M. tuberculosis* and lesser sequence similarity to members of the plant peroxidase family (Carpena *et al.*, 2002). In 2003, the 1.7 Å crystal structure of BpKatG was described (Carpena *et al.*, 2003). The crystallized enzyme shows that BpKatG is a homodimer of 79 kDa subunits with one modified heme group and one metal ion, likely sodium, per subunit. Each subunit has distinct N- and C-terminal domains that are structurally related and similar to plant peroxidases. The heme environment of BpKatG is similar to that of plant peroxidases. On the distal side of the heme, the active-site triad of Arg 108, Trp111 and His112 is typical of all catalase-peroxidases and of class I peroxidases. On the proximal side, His279 is the fifth ligand to the heme iron atom as the peroxidases, and it is in close association with fully conserved Asp389, which interacts with the indole N atom from the proximal Trp330 (Carpena *et al.*, 2003).

#### **1.5.1. The unusual covalent modifications**

The electron density maps of BpKatG presented two unusual covalent modifications. A covalent adduct structure linked the active site Trp111 with Tyr238 and Tyr238 with Met264, and the heme was modified likely by a perhydroxy group added to the vinyl group on the ring I (Carpena *et al.*, 2003).

### 1.5.1.a. A covalent adduct structure linked Trp111-Tyr238-Met264

The structure of covalent adduct, also found in the crystal structure of HmCPx (Yamada *et al.*, 2001), involves the indole ring of the active site Trp111 and the sulfur of Met264 joined to the ortho positions of Tyr238 ring. It was found in close proximity to a modification on the heme. The Trp111 component is a catalytic residue required for compound I reduction in catalatic reaction (Hillar *et al.*, 2000 and Jakopitsch *et al.*, 2003). The possible roles for the covalent adduct include stabilizing the indole ring in the active site and providing a route for electron transfer. The evidence obtained from mass spectrometry analyses of BpKatG, *E. coli* HPI (Donald *et al.*, 2003), and the *Synechocystis* KatG (Jakopitch *et al.*, 2003) have confirmed the presence of the Trp-Tyr-Met adduct in four catalase-peroxidases and supports the conjecture that the structure may be common to all catalase-peroxidases (Chelikani *et al.*, 2003). The active site Trp from *E. coli* HPI (Hillar *et al.*, 2000) and the *Synechocystis* KatG (Regelsberger *et al.*, 2000 and 2001) is essential for normal catalatic activity, but not peroxidatic activity. The replacement of Trp by Phe results in the loss of catalase activity, but enhanced peroxidase activity. Subsequent studies have shown that replacement of either Met264 (Donald *et al.*, 2003) or Tyr238 (Jakopitch *et al.*, 2003) have a similar effect in eliminating catalase activity with no effect or a positive effect on peroxidase activity. This suggests that the complete cross-linked structure is required for catalatic activity but not for peroxidatic activity, providing a clear explanation for why the apparently closely related plant peroxidases have no, or only a trace, of catalase activity. A free radical mechanism involving hydrogen peroxide as an oxidant has been proposed for the creation of the cross-linked structure among Trp111, Tyr238 and Met264 (Chelikani *et al.*, 2003).

### **1.5.1.b. Heme modification**

A second unusual modification in BpKatG, not evident in HmCPx structure, is an apparent perhydroxy modification on the ring I vinyl group of the heme. The modification could arise from a simple hydration-like addition of hydrogen peroxide across the double bond of the vinyl group. It is shown to be removed easily by treatment of the enzyme with INH, a peroxidatic substrate (X. Carpena, personal communication). The function of the perhydroxy group could be a reservoir of H<sub>2</sub>O<sub>2</sub> in the active site, available for immediate reaction when a peroxidatic substrate is contacted (Chelikani et al., 2003).

### **1.5.2. Substrate access channel**

There are at least two channels that provide access to the active site. Despite the apparent structural similarity to plant peroxidases, the larger subunit size of BpKatG (more than twice as large) results in the active site of BpKatG, including the resident heme, being buried more deeply within the subunit. The most obvious access route of the enzyme to the distal side of the heme, the active site of the enzyme for reaction with H<sub>2</sub>O<sub>2</sub>, is provided by a channel positioned similarly to, but longer than, the access route in peroxidases. The channel in BpKatG has a pronounced funnel shape that approaches the heme laterally and is narrowest near residues Ser324 and Asp141, about 14 Å from the heme iron atom. In peroxidases, the channel is not as constricted, and the peroxidatic substrate, benzhydroxamic acid, binds to horseradish peroxidase (HRP) in a position that is more constricted in BpKatG. Substrate hydrogen peroxide entering the distal side cavity of BpKatG through the constricted portion of the channel would immediately

come into contact with the active site residues Arg108, Trp111 and His112 for generation of compound I in both the catalytic and peroxidatic reactions, or for the reduction of compound I in the catalytic reaction. A region of undefined electron density located just before the constricted region in this channel was observed. The location of the density is over 10 Å further away from the heme than is the benzhydroxamic acid bound in HRP, but is in close proximity to Ser324, the equivalent of Ser315 in MtKatG, which is thought to be involved in INH binding because changing it interferes with INH activation.

Another funnel-shaped access channel approaches a small central cavity containing a single metal ion, which was tentatively identified as sodium on the basis of its refinement properties and pentavalent, square pyramidal coordination structure with distances of about 2.35 Å. It is coordinated to the carbonyl oxygen atom of residues 122, 124 and 494 as well as two water molecules. The second channel provides direct access to the core of the protein and to a region that encompasses two other structural features with possible functional significance. The first is a large cleft in the side of the subunit formed between two domains of the subunit that wraps around the protein, which is evident and may be a potential substrate-binding site with a clear pathway for electron transfer to the active site heme group through the adduct. A second feature is the side-chain of Arg426, which exists in two orientations, of which the predominant (>70%) differs from the orientation in HmCPx. Contributing to the complexity of this region are the two conformations of the side-chain of Thr119, of which the minor (<30%) is similar to the conformation in HmCPx, suggesting coordination between the conformations of the two side-chains. Changes relative to HmCPx (the single ion, the rotated Asp427

carbonyl group, and the displaced Thr119 and Arg426 side-chains) are in close proximity to one another, are associated directly or indirectly through hydrogen bonds or ionic interactions and represent the only changes in structure relative to HmCPx in this region of the protein. This correlation suggests strongly that the changes are functionally related, and that the region of the protein may have an, as yet, undefined function, possibly as a second catalytic center besides the heme. This possibility is reinforced by the fact there is a region of undefined electron density located in the cavity vacated by the Arg426 side-chain in direct contact with the oxygen atom of the side-chain from Tyr238, the central residue of the covalent adduct (Carpena et al., 2003).

## **1.6. Objectives of thesis**

The objective of this thesis is to confirm the catalytic and structural roles of highly conserved active site residues, Arg108, His112 and Asp141 of catalase-peroxidase KatG from *Burkholderia pseudomallei* by using site-directed mutagenesis methodology (Figure 1.1). The BpKatG variants will be characterized for catalase activity, peroxidase activity, NADH oxidase activity, INH hydrazinolysis activity, kinetic parameters and sensitivity to common heme-binding inhibitors. It is expected that these data will provide important information about the role of these residues.

1 MPGSDAGPRR RGVHEQRRNR MSNEAKCPFH QAAGNGTSNR  
 41 DWWPNQLDLS ILHRHSSLSD PMGKDFNYAQ AFEKLDLAAV  
 81 KRDLHALMTT SQDWWPADFG HYGGLFIRMA WHSAGTYRTA  
 121 DGRGGAGEGQ QRFAPLNSWP DNANLDKARR LLWPIKQKYG  
 161 RAISWADLLI LTGNVALESM GFKTFGFAGG RADTWEPEDV  
 201 YWGSEKIWLE LSGGPNSRYS GDRQLENPLA AVQMGLIYVN  
 241 PEGPDGNPDP VAAARDIRDT FARMAMNDEE TVALIAGGHT  
 281 FGKTHGAGPA SNVGAEPEAA GIEAQGLGWK SAYRTGKGAD  
 321 AITSGLEVTW TTTPTQWSHN FFENLFGYEW ELTKSPAGAH  
 361 QWVAKGADAV IPDAFDPSKK HRPTMLTTDL SLRFDPAYEK  
 401 ISRRFHENPE QFADAFARAW FKLTHRDMGP RARYLGPEVP  
 441 AEVLLWQDPI PAVDHPLIDA ADAAELKAKV LASGLTVSQL  
 481 VSTAWAAAST FRGSDKRGA NGARIRLAPQ KDWEANQPEQ  
 521 LAAVLETLEA IRTAFNGAQR GKGQVSLADL IVLAGCAGVE  
 561 QAAKNAGHAV TVPFAPGRAD ASQEQT DVES MAVLEPVADG  
 601 FRNYLKGKYR VPAEVLLVDK AQLLTLSAPE MTVLLGGLRV  
 641 LGANVGQSRH GVFTAREQAL TNDFVFNLLD MGTEWKPTAA  
 681 DADVFEGRDR ATGELKWTGT RVDLVFGSHS QLRALAEVYG  
 721 SADAQEKFVR DFVAVWNKVM NLD RFDLA

**Figure 1.1.** Amino acid sequence of catalase-peroxidase BpKatG. The underlined letters are the amino acids that have been modified.

## 2. MATERIALS AND METHODS

### 2.1. *Escherichia coli* strains, plasmids and bacteriophage

The *E. coli* strains, plasmids and bacteriophage used in this study are listed in Table 2.1. Phagemid pKS- from Stratagene Cloning Systems was used as a vector for mutagenesis, sequencing and cloning. The *Burkholderia pseudomallei* *katG* gene, encoding catalase-peroxidase BpKatG, was inserted into plasmid pKS- to generate the plasmid pBpG. Strain CJ236, harbouring plasmids pBpG-KC, containing subcloned fragment II of the *B. pseudomallei* *katG* gene (Figure 2.1) was used for generation of single-stranded, uracil-containing DNA templates employed for site-directed mutagenesis. Helper phage R408 was used for infection of the strain CJ236 to generate single-stranded DNA. Strain NM522 was used for cloning and plasmid propagation. Strain JM109 was used for production of plasmid DNA for double-stranded DNA sequencing. Strain UM262, which is catalase negative was used for routine expression of variant proteins.

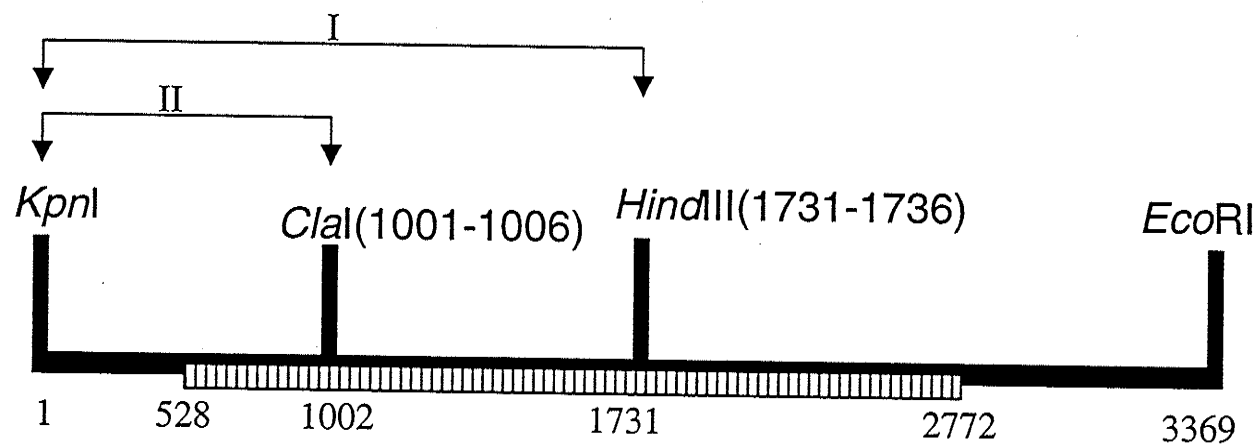
### 2.2. Biochemical and common reagents



All biochemicals and reagents, as well as antibiotics used in the course of these studies, were purchased from either Sigma Chemical Co. (St. Louis, Missouri), or from Fisher Scientific Ltd. (Mississauga, Ontario). Restriction nucleases, polynucleotide kinase, T4 DNA ligase and most other enzymes used in these studies were purchased



**Table 2.1.** List of *Escherichia coli* strains, plasmids and bacteriophage used in this study.

Genotype or characteristics		Source
<b><u>E. coli strains</u></b>		
CJ236	<i>dut1 ung1 thi-1 relA1/pCJ105/cam<sup>r</sup>F'</i>	Kunkel <i>et al.</i> , 1987
NM522	<i>supE Δ(lac-proAB) hsd-5 [F' proAB lacI<sup>q</sup> lacZΔ15]</i>	Mead <i>et al.</i> , 1985
JM109	<i>recA1 supE44 endA1 hsdA1 hsdR17 gyrA96 relA1 thi Δ(lac-proAB)</i>	Yanisch-Perron <i>et al.</i> , 1985
UM262	<i>recA katG::Tn10 pro leu rpsL hsdM hsdR endI lacY</i>	Loewen <i>et al.</i> , 1990
<b><u>Plasmids</u></b>		
pKS-	Amp <sup>R</sup>	Stratagene Cloning Systems
pBpG (pKS-, <i>B. pseudomallei</i> <i>katG</i> clone)	Amp <sup>R</sup>	This study
pBpG-KH (pKS-, subclone I)	Amp <sup>R</sup>	This study
pBpG-KC (pKS-, subclone II)	Amp <sup>R</sup>	This study
<b><u>Bacteriophage</u></b>		
R408 (helper phage)		Stratagene Cloning Systems



**Figure 2.1.** Simplified restriction map of the chromosomal insert containing the *B. pseudomallei katG* gene in plasmids pBpG, pBpG-KH (Fragment I) and pBpG-KC (Fragment II). The 1134 bp long *katG* open reading frame  is indicated as part of the chromosomal insert  as are the two insert fragments I and II used to construct the subclone vectors employed in site-directed mutagenesis of *B. pseudomallei katG*.

from Invitrogen Canada Inc. (Burlington, Ontario). The T7 sequencing kit was purchased from USB Corporation (Cleveland, Ohio). Components for the media used for growth of bacteria cell cultures were purchased from DIFCO (U.S.A.). Solutions were prepared using reverse osmosis distilled water.

### **2.3. Media, growth conditions and storage of cultures**

*E. coli* cultures were usually grown in LB (Luria-Bertani) medium containing 10 g/L tryptone, 5 g/L yeast extract, and 5 g/L NaCl. Solid LB media contained 15 g/L agar. Ampicillin was added to a concentration of 100 µg/ml for maintenance of selection pressure on plasmid-harboring strains grown in both liquid and solid media. In addition, chloramphenicol was added to a concentration of 40 µg/ml in order to maintain the presence of F' episome for the growth of the strain CJ236.

*E. coli* strains in general were grown in solid or liquid media at 37°C. However, cell cultures in liquid media for expression of wild type and variant proteins were grown at either 28°C or at 37°C in shake flasks with good aeration depending on what was optimum for a particular variant. Long term storage of stock cultures was in 24% dimethylsulfoxide (DMSO) at -60°C. Bacteriophage R408 was stored at 4°C in LB culture supernatant.

## 2.4. DNA manipulation

### 2.4.1. Preparation of synthetic oligonucleotides

The oligonucleotides used for site-directed mutagenesis were purchased from Invitrogen (Burlington, Ontario) in non-phosphorylated form. The concentration of oligonucleotide DNA was determined spectrophotometrically at 260 nm, where 1 unit of absorbance  $\approx$  20  $\mu$ g/ml single-stranded DNA (Sambrook *et al.*, 1989).

Oligonucleotides used for site-directed mutagenesis were phosphorylated at the 5'-ends using T4 kinase (Invitrogen Canada Inc.) according to the procedure of Ausubel *et al.* (1989). Approximately 100 ng of oligonucleotide DNA in a volume of 25  $\mu$ l, containing 1 mM ATP and 10 units of kinase were incubated in appropriately diluted buffer supplied by the manufacturer at 37°C for 30 minutes. The reaction was terminated by heat inactivation at 65°C for 5 minutes.

### 2.4.2a. Site-directed mutagenesis strategy

Targeted base changes on phagemid-borne *B. pseudomallei katG* were generated according to the *in vitro* mutagenesis protocol described by Kunkel *et al.* (1987). Subclones were constructed from parts of the chromosomal insert containing the *katG* gene on pKS-. A simplified restriction map of *BpkatG* gene indicating the locations of individual subclones is shown in figure 2.1 The subclone rather than the whole gene was mutagenized in order to limit the amount of subsequent sequencing required to confirm mutation in the subclone both after mutagenesis and after reinsertion into the *BpkatG* gene for protein expression. Target codons for mutagenesis were selected from the DNA

sequence of *BpkatG* gene shown in figure 2.3. DNA sequences for oligonucleotides used in the mutagenesis procedure are listed in Table 2.2. Mutagenesis was performed by annealing the phosphorylated oligonucleotides encoding the desired base modifications to uracil-containing single-stranded DNA templates obtained from the appropriate Bluescript phagemid subclone. The complementary DNA strand was then synthesized *in vitro* by unmodified T7 DNA polymerase (New England Biolabs) using the annealed oligonucleotide as a primer. The 3' and 5' ends of the completed complementary strand were ligated by adding T4 DNA ligase (Invitrogen Canada Inc.) in the reaction mixture. The DNA was then transformed into NM522 cells where the uracil-containing templates were degraded. Plasmid DNA recovered from the transformants was further transformed into JM109, recovered from this strain and used to screen for the desired mutation in the plasmid subclone by DNA sequencing. Once the correct mutant was identified, the complete subclone sequence was determined in order to ensure that no base changes apart from those desired had been introduced. The mutated subclone was then used to reconstruct the complete *BpkatG* gene, which was then sequenced over the region containing the mutation for final confirmation. Reconstructed, mutant *BpkatG* clones were then transformed into UM262 for determination of enzyme activities and visualization of protein from crude extracts or whole cells by SDS-PAGE. Clones expressing significant levels of variant BpKatG enzyme were then grown on a large scale (4-6 liters) for purification and characterization of the enzyme.

### 2.4.2b. Reconstruction of *B. pseudomallei* *katG* subclones with desired mutation

An outline of the reconstruction protocol is illustrated in Figure 2.2. The plasmids have been drawn in a linearized form for reasons of simplicity. Reconstruction of mutant *katG* genes involved two stages. In the first stage, plasmid pBpG-KC (subclone I) with the desired mutation was cut with *KpnI* and *ClaI*. The 1002 bp *KpnI*-*ClaI* fragment from pBpG-KC (subclone I) was then ligated into pBpG-KH (subclone II) that was also cut with *KpnI* and *ClaI*. In the second stage; plasmid pBpG-KH (subclone II) with the desired mutation was cut with *KpnI* and *HindIII*. The 1731 bp *KpnI*-*HindIII* fragment from pBpG-KH (subclone II) was then ligated into pBpG that was also cut with *KpnI* and *HindIII* to generate the plasmid containing mutant *katG* gene. All the variant constructs were verified for correct restriction sites using various restriction digestion studies at each step in the construction process.

### 2.4.3. DNA isolation and purification

Plasmid DNA was isolated according to Sambrook *et al.* (1989). All procedures were carried out at 4°C. Plasmid containing cells from 5 ml LB cultures grown to stationary phase were pelleted by centrifugation and resuspended in 200 µl glucose-EDTA buffer (25 mM Tris-HCl, pH 8.0, 1% glucose, 10 mM Na-EDTA). The cells were then lysed by addition of 400 µl 1% SDS (w/v), 0.2 M NaOH solution and gently mixed. This was then neutralized by addition of 300 µl of 6.2 M ammonium acetate, pH 5.9. After 10 minutes incubation on ice, the mixture was centrifuged twice to remove all precipitates. Plasmid DNA was then precipitated by addition of 550 µl isopropanol to the remaining supernatant followed by a 15-minutes incubation at room temperature. It was

**Table 2.2.** Sequences of oligonucleotides used for site-directed mutagenesis of *Burkholderia pseudomallei katG*.

Primer name	Base change	Oligonucleotide sequence <sup>a</sup>
R108A	CGC → GCC	CTGTT <b>CATCGCC</b> ATGGCATGG
R108K	CGC → AAA	CTGTT <b>CATCAAA</b> ATGGCATGG
H112A	CAC → GCC	ATGGCATGG <b>GCC</b> AGCGGGCAC
H112N	CAC → AAC	ATGGCATGG <b>AAC</b> AGCGGGCAC
D141A	GAC → GCC	AGCTGGCC <b>CGCCA</b> ACGCGAAC
D141E	GAC → AAC	AGCTGGCC <b>CAACA</b> ACGCGAAC
D141N	GAC → GAA	AGCTGGCC <b>CGAAA</b> ACGCGAAC

<sup>a</sup>The sequences in bold are the codons that have been modified

**Figure 2.2.** General reconstruction protocol used for generation of variant *katG*'s from mutagenized subclone I for protein expression. (K:*Kpn*I, C:*Cla*I, H:*Hind*III, E:*Eco*RI)

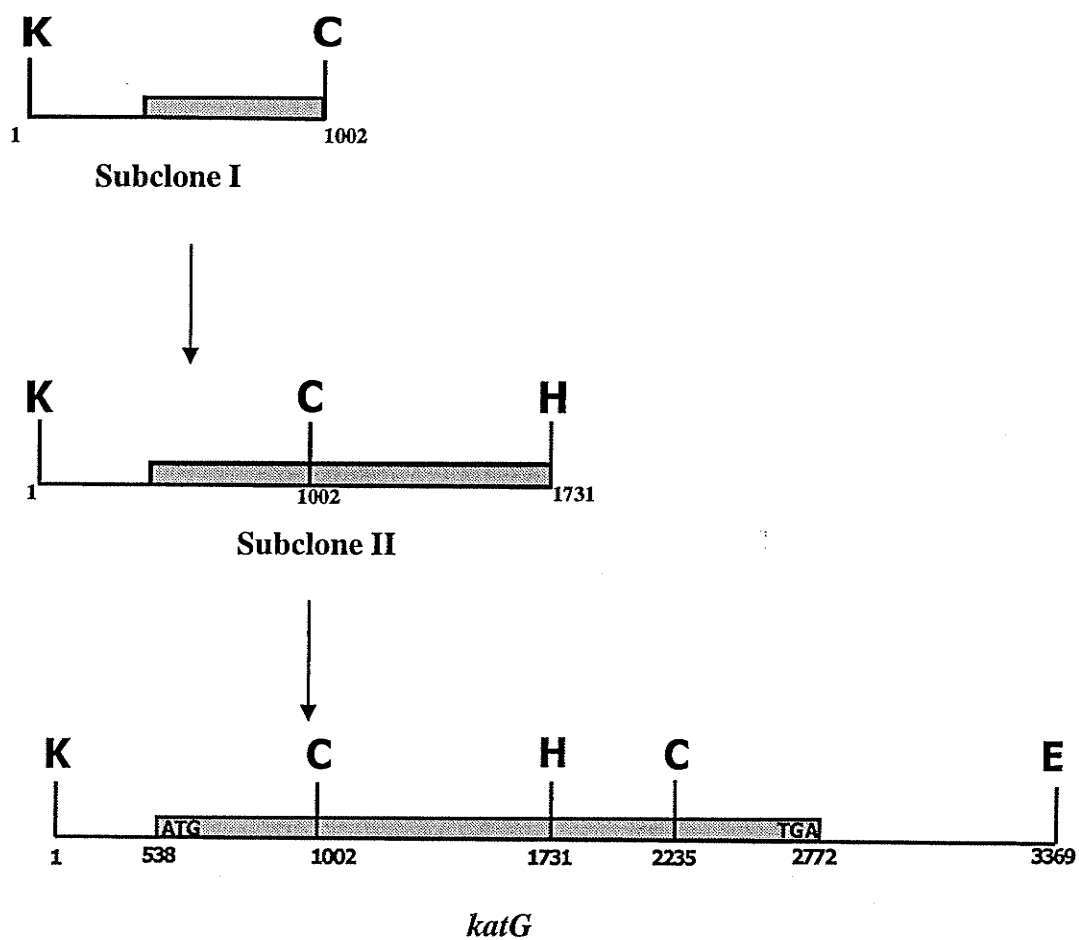




**Figure 2.3.** Nucleotide sequence of *Burkholderia pseudomallei* *katG* showing the restriction sites, the sequencing primers (BpG 1-6) and mutagenic oligonucleotides indicating base changes.

```

CGGGGTGACGAAGCTCGATATCCCGGCGACGGTGAATTGAGCGCGGCGAGCGCAGCTG      60
GCCCCACTGCTTCGAGCTATAGGGCCGCTGCCACTTAACTCGCGCCGCTCGCGACGAC

CGGGCCGCGCGCGCCATGATCGGACGGGGCTTCGGGGCCCCGTTTATTTTTGCCTATCG      120
GCCCCGCGGCGCGCGGTACTAGCCTGCCCCGAAGCCCCGGGGCAAATAAAAACGGATAGC

GATAAATAAAATTTATTAAATTACATATATCAATAGCAAATAATAGAATGCTTCGCATGG      180
CTATTTATTTTAAATAATTTAATGTATATAGTTATCGTTTATTATCTTACGAAGCGTACC

ATCGGCGCAGCGCCGCCGGACGGTAACTGCAAGCGTCAAGGGAGGATGTCATGATGCAAC      240
TAGCCGCGTCGCGGCGGCCTGCCATTGACGTTTCGAGTTCCCTCCTACGTAAGTACGTTG

CGGCATTGTGCGCGCGCGGGCGGAACATTGCGCCGCGCCCGGCGGTCATTGATCGTGCCA      300
GCCGTAACAGCGCGCGCGCCGCTTGTAAACGCGGCGCGGGCCGCCAGTAACTAGCACGGT

AGGCTGCCATCCGGAGCCTGCGTCCGATTGCGTTGCTTATCTGGCGGACCGCGCCACG      360
TCCGACGGTAGGCCACGGACGCAGGCTAACGCAAGCGAATAGACCGCCTGGCGCGGGTGC

GCGGCTGAGCGCCGCGCGTGCCGGGCGCTTTTTTCGCGCCGCGCGTCGCGTCGCACGC      420
GCCCGACTCGCGGCGGCGCACGGCCCGGCGAAAAAAGCGCGGCGCGCAGCGCAGCGTGCG
-----

                                     M P G S      (4)
AGGAGGGGTCAACCTGTTTGTTCCTCCCGCAAAGTCGCCCCCGAACGATGCCCCGGCTCCG      480
TCCTCCCCAGTTGGACAAACAAAGGGGCGTTTCAGCGGGGGGCTTGCTACGGGCCGAGGC
----->BpG2
----->BpG5

G A G P R R R G V H E Q R R N R M S N E      (24)
ATGCCGGGCCCCGAGGCGGGGCGTACACGAACAAAGGAGAAATCGCATGTGCAATGAAG      540
TACGGCCCCGGGCGTCCGCCCCGCATGTGCTTGTTCCTCTTTAGCGTACAGCTTACTTC

A K C P F H Q A A G N G T S N R D W W P      (44)
CGAAGTGCCCGTTCCATCAAGCCGCAGGCAACGGCACGTGCAACCGGGACTGGTGGCCCA      600
GCTTCACGGGCAAGGTAGTTTCGGCGTCCGTTGCCGTGCAGCTTGGCCCTGACCACCGGGT

N Q L D L S I L H R H S S L S D P M G K      (64)
ATCAGCTGGACCTGAGCATCCTGCATCGGCACTCGTCGTGTCGATCCGATGGGCAAGG      660
TAGTCGACCTGGAAGCTAGGACGTAGCCGTGAGCAGCGACAGGCTAGGCTACCCGTTCC

D F N Y A Q A F E K L D L A A V K R D L      (84)
ATTTCAACTACGCGCAGGCGTTTCGAGAAGCTCGACCTCGCGGCGGTGAAGCGCGACCTCC      720
TAAAGTTGATGCGCGTCCGCAAGCTCTTCGAGCTGGAGCGCCGCACTTCGCGCTGGAGG

```

H A L M T T S Q D W W P A D F G H Y G G (104)  
 ACGCGCTGATGACGACGTGCGAGGACTGGTGGCCGGCCGATTTCGGCCACTACGGCGGCC 780  
 TCGCGACTACTGCTGCAGCGTCCTGACCACCGCCGGCTAAAGCCGGTGATGCCGCCGG  
 ----->BpG6

L F I R M A W H S A G T Y R T A D G R G (124)  
 TGTTTCATCCGCATGGCATGGCACAGCGCGGGCACGTACCGCACGGCCGACGGCCGCGGCG 840  
 ACAAGTAGGCGTACCGTACCGTGTGCGCGCCGTGCATGGCGTGCCGGCTGCCGGCGCCGC  
 -----AAA----- R108K  
 -----GCC----- R108A  
 -----GCC----- H112A  
 -----AAC----- H112N

G A G E G Q Q R F A P L N S W P D N A N (144)  
 GCGCGGGCGAAGGGCAGCAGCGCTTCGCGCCGCTCAACAGCTGGCCCGACAACGCGAACC 900  
 CGCGCCCGCTTCCCGTCGTGCGAAGCGCGGCGAGTTGTCGACCGGGCTGTTGCGCTTGG  
 -----GCC----->D141A  
 -----AAC----->D141N  
 -----GAA----->D141E

L D K A R R L L W P I K Q K Y G R A I S (164)  
 TCGACAAGGCGCGCCGGCTGCTGTGGCCGATCAAGCAGAAGTACGGCCGCGCCATCTCGT 960  
 AGCTGTTCCGCGCGGCCGACGACACCGGCTAGTTTCGTCTTCATGCCGGCGCGGTAGAGCA

W A D L L I L T G N V A L E S M G F K T (184)  
 GGGCCGACCTGCTGATCCTGACGGGCAACGTGCGGCTCGAATCGATGGGCTTCAAGACCT 1020  
 CCCGGCTGGACGACTAGGACTGCCCGTTGCAGCGCGAGCTTAGCTACCCGAAGTTCTGGA  
*ClaI*

F G F A G G R A D T W E P E D V Y W G S (204)  
 TCGGCTTCGCGGGCGGCCGCGCGGACACGTGGGAGCCCGAGGACGTCTACTGGGGCTCGG 1080  
 AGCCGAAGCGCCCGCGGCGCGCTGTGCACCTTCGGGCTCCTGCAGATGACCCCGAGC

E K I W L E L S G G P N S R Y S G D R Q (224)  
 AAAAGATCTGGCTGGAAGTGAAGCGGCGGCCGAACAGCCGCTATTCGGGCGACCGCCAGC 1140  
 CTTTTCTAGACCGACCTTGACTCGCCGCCGGCTTGTGCGCGATAAGCCCGCTGGCGGTG

L E N P L A A V Q M G L I Y V N P E G P (244)  
 TCGAGAACCCGCTCGCCGCCGTGCAGATGGGCTCATCTACGTGAATCCGGAAGGCCCGG 1200  
 AGCTCTTGGGCGAGCGGCGGCACGTCTACCCGGAGTAGATGCACTTAGGCCTTCCGGGGC

D G N P D P V A A A R D I R D T F A R M (264)  
 ACGGCAATCCCGATCCGGTCGCCGCGGCGCGGACATTGCGTACACCTTCGCGCGCATGG 1260  
 TGCCGTTAGGGCTAGGCCAGCGGCGCCGCGCGCTGTAAGCACTGTGGAAGCGCGCGTACC

A M N D E E T V A L I A G G H T F G K T (284)  
 CGATGAACGACGAAGAGACGGTCGCGCTGATCGCGGGCGGCCACACGTTCCGGAAGACGC 1320  
 GCTACTTGCTGCTTCTCTGCCAGCGCGACTAGCGCCCGCCGGTGTGCAAGCCGTTCTGCG  
 ----->BpG3

H G A G P A S N V G A E P E A A G I E A (304)  
 ACGGCGCGGGGCGCGTCAACGTGCGCGCCGAGCCGGAGGCCGCGGGCATCGAAGCGC 1380  
 TGCCGCGCCCCGGGCGCAGCTTGACGCCGCGGCTCGGCCTCCGGCGCCCGTAGCTTCGCG

Q G L G W K S A Y R T G K G A D A I T S (324)  
 AGGGCCTCGGCTGGAAGAGCGCGTACCGCACGGGCAAGGGCGCGGACGCGATCACGAGCG 1440  
 TCCCGAGCCGACCTTCTCGCGCATGGCGTGCCCGTTCCCGCGCCTGCGCTAGTGCTCGC

G L E V T W T T T P T Q W S H N F F E N (344)  
 GGCTCGAAGTCACGTGGACGACGACGCCGACGAGTGGAGCCACAATTCTTCGAGAACC 1500  
 CGGAGCTTCAGTGCACCTGCTGCTGCGGCTGCGTCACCTCGGTGTTGAAGAAGCTCTTGG

L F G Y E W E L T K S P A G A H Q W V A (364)  
 TGTTCCGGCTACGAGTGGGAGCTGACGAAGAGCCCGGGCGGGCGCGACCAAGTGGGTGCGA 1560  
 ACAAGCCGATGCTCACCTCGACTGCTTCTCGGGCCGCCGCGCGTGGTCACCCAGCGCT

K G A D A V I P D A F D P S K K H R P T (384)  
 AGGGCGCCGACGCGGTGATTCCCGACGCGTTTCGATCCGTGCAAGAAGCATCGTCCGACGA 1620  
 TCCCGCGGCTGCGCCACTAAGGGCTGCGCAAGCTAGGCAGCTTCTTCGTAGCAGGCTGCT

M L T T D L S L R F D P A Y E K I S R R (404)  
 TGCTCACGACCGACCTGTGCTGCGCTTCGATCCGGCGTACGAAAAGATCTCGCGCCGCT 1680  
 ACGAGTGCTGGCTGGACAGCGACGCGAAGCTAGGCCGCATGCTTTTCTAGAGCGCGGCGA

F H E N P E Q F A D A F A R A W F K L\* T (424)  
 TCCACGAGAACCCGGAGCAGTTGCGCGACGCGTTGCGCGCGCCTGGTTCAAGCTTACGC 1740  
 AGGTGCTCTTGGGCTCGTCAAGCGGTGCGCAAGCGCGCGGGACCAAGTTCGAGTGCG  
 -----T-----  
 HindIII

H R D M G P R A R Y L G P E V P A E V L (444)  
 ACCGCGACATGGGCCCCGCGCGCGCTATCTCGGCCCCGGAAGTGCCGGCCGAGGTGCTGC 1800  
 TGGCGCTGTACCCGGGCGCGCGCGCATAGAGCCGGGCCCTTACGGCCGGCTCCACGACG  
 -->BpG1

L W Q D P I P A V D H P L I D A D A A A (464)  
 TGTGGCAGGACCCGATTCCGGCCGTCGACCATCCGCTGATCGACGCCGCGGACGCCGCCG 1860  
 ACACCGTCTCTGGGCTAAGGCCGGCAGCTGGTAGGCGACTAGCTGCGGCGCCTGCGGCGGC

E L K A K V L A S G L T V S Q L V S T A (484)  
 AGCTGAAGGCAAAGGTGCTCGCGTCGGGGCTGACCGTGTCGCGAGCTCGTTTCCACCGCGT 1920  
 TCGACTTCCGTTTCCACGAGCGCAGCCCCGACTGGCACAGCGTCGAGCAAAGGTGGCGCA

W A A A S T F R G S D K R G G A N G A R (504)  
 GGGCGGCGGCGTCCACCTTCCGCGGCTCGGACAAGCGCGGCGGCGCAACGGCGCGCGCA 1980  
 CCCGCCGCGCAGGTGGAAGGCGCCGAGCCTGTTGCGCGCGCGCGCTTGCCGCGCGCGT

I R L A P Q K D W E A N Q P E Q L A A Y (524)  
 TTCGCTTGCGCCGAGAAGGACTGGGAGGCGAACCAGCCCCGAGCAGCTCGCGGCGGTGC 2040  
 AAGCGGAACGCGGCGTCTTCTGACCCTCCGCTTGGTCGGGCTCGTCGAGCGCCGCCACG

L E T L E A I R T A F N G A Q R G G K Q TCGAGACGCTCGAGGCAATTCGCACGGCGTTCAACGGCGCGCAGCGCGGCGGCAAGCAAG AGCTCTGCGAGCTCCGTTAAGCGTGCCGCAAGTTGCCGCGCGTCGCGCCGCGTTTCGTTT	(544) 2100
V S L A D L I V L A G C A G V E Q A A K TGTCGCTCGCCGATCTGATCGTGCTGGCCGGCTGCGCGGGCGTCGAGCAGGCGGCGAAGA ACAGCGAGCGGCTAGACTAGCACGACCGGCCGACGCGCCCGCAGCTCGTCCGCGCTTCT	(564) 2160
N A G H A V T V P F A P G R A D A S Q E ACGCGGGCCACGCGGTGACCGTGCCGTTGCGCGCGGGCCGCGCGGACGCATCGCAGGAGC TGCGCCCGGTGCGCCACTGGCACGGCAAGCGCGGCCCGGCGCGCCTGCGTAGCGTCCTCG	(584) 2220
Q T D V E S M A V L E P V A D G F R N Y AGACCGACGTGCAATCGATGGCCGTGCTCGAGCCGGTGGCCGACGGTTTTTCGCAACTACC TCTGGCTGCAGCTTAGCTACCGGCACGAGCTCGGCCACCGGTGCCAAAAGCGTTGATGG <i>C7aI</i>	(604) 2280
L K G K Y R V P A E V L L V D K A Q L L TGAAGGGCAAGTATCGGGTGCCCGCCGAGGTGCTGCTCGTCGACAAGGCGCAACTGCTGA ACTTCCCGTTCATAGCCACGGGCGGCTCCACGACGAGCAGCTGTTCCGCGTTGACGACT	(624) 2340
T L S A P E M T V L L G G L R V L G A N CGCTGAGCGCGCCGGAGATGACGGTGCTGCTGGGCGGCCTGCGCGTGCTGGGCGCGAACG GCGACTGCGCGGCCCTCTACTGCCACGACGACCCGCCGGACGCGCACGACCCGCGCTTGC	(644) 2400
V G Q S R H G V F T A R E Q A L T N D F TCGGGACAGAGCCGGCACGGCGTGTTACCGCGCGCGAGCAGGCATTGACCAACGACTTCT AGCCCGTCTCGGCCGTGCCGCACAAGTGCGCGCGCTCGTCCGTAAGTGGTTGCTGAAGA	(664) 2460
F V N L L D M G T E W K P T A A D A D V TCGTGAACCTGCTCGACATGGGCACCGAGTGGAAGCCGACGGCGGCCGACGCGGACGTGT AGCACTTGGACGAGCTGTACCCGTGGCTCACCTTCGGCTGCCGCCGGCTGCGCCTGCACA	(684) 2520
F E G R D R A T G E L K W T G T R V D L TCGAAGGGCGCGACCGCGCGACGGGCGAGCTCAAGTGGACGGGCACGCGCTCGATCTCG AGCTTCCCGCGCTGGCGCGCTGCCCGCTCGAGTTCACCTGCCCGTGCGCGCAGCTAGAGC	(704) 2580
V F G S H S Q L R A L A E V Y G S A D A TGTTCCGGCTCGCACTCGCAGTTGCGCGCGCTCGCGGAGGTCTACGGCAGCGCGGACGCGC ACAAGCCGAGCGTGAGCGTCAACGCGCGCGAGCGCCTCCAGATGCCGTGCGCCTGCGCG	(724) 2640
Q E K F V R D F V A V W N K V M N L D R AGGAGAAGTTTCGTGCGCGACTTCGTGCGGGTCTGGAACAAGGTGATGAACCTCGACCGCT TCCTCTTCAAGCACGCGCTGAAGCAGCGCCAGACCTTGTTCCACTACTTGGAGCTGGCGA	(744) 2700
F D L A * TCGATCTGCGGTGATCGCGCCGCGCGCCGCGGAGCGGCGGCGCGCGGCGGCGGGGAAC AGCTAGAGCGCACTAGCGCGGCGGCGCGGCGGCTCGCCGCCGCGCGCCGCCGCCCTTG	(748) 2760

BpG4&lt;-----

GGCCGGCTGACGCGGGCCGCTTCCCGCCGGGCGCTGATATCGTTTCAAGGAGTGACGAT	2820
CATGACGCAAATGATTCTCGACCTGCGCGGGGCGCTCGCGGGCGCCGGCCAGGCGCGCGGG	2880
CGCCGCGGGCGTGGCGGGCGGCTGATCGGCCTCGCGATCGCGGGCGGCGGCGGCGCGTGT	2940
GGCCGCGCAGGCCGCGCGCTACTTCACGGCGGGCGCCGGCGGTTGAGCGGGCCTGCGTTT	3000
CGCGCAAATCGCGCGCTCGCGATCTACGCTAACTGGTGCGGCGCTCGGCGGGCAGCCGC	3060
ACGCGCGTCTGCCGCCTCTGCATAGGCTGCCCATGCGCATGTCGCCTGCGCGCATCCCGC	3120
ATCGGGCATGCGGATCTTTTCGATGCATTTTCGTGCGTTTGAACCATCGGACAAGGAGTTT	3180
CGAGGATGGCCAAGAAAAGCAACGCAACCCAGATCAACATCGGCATCAGCGACAAGGATC	3240
GCAAGAAGATCGCGGCGGGGCTGTCGCGTCTGCTCGCCGATACGTACACGCTGTACCTGA	3300
AGACGCACAATTTCCACTGGAACGTGACCGGCCCCGATGTTCAACACGCTGCACCTGATGT	3360
TCGAGGAGCAGTACAACGAACTGTGGCTCGCCGTCGATCTCGTCGCGGAGCGCATCCGCA	3420
CGCTCGGGGTCGTCGCGCCGGGACGATATCGCGAATTCGCGAAGCTGTCGTCGATTCCCG	3480
AGGCCGACGGCGTGCCGGCCGCCGAGGAGATGATTCGCCAGCTCGTCGAAGGGCATGAGG	3540
CTGTGTCGCGCACCGCGCGCGGATCTTCCCGGACGCCGACGCGGCGAGCGACGAGCCCA	3600
CCGCCGATCTGCTGACGCAGCGCCTGCAG	3629

then pelleted by centrifugation, washed twice with 70% (v/v) ice-cold ethanol, and then dried under vacuum. The DNA pellet was either stored in this condition at  $-20^{\circ}\text{C}$  or was suspended in HPLC grade water or TE buffer (10 mM Tris, pH 8.0, 1 mM Na-EDTA) prior to storage at  $-20^{\circ}\text{C}$  until further use.

Single-stranded template DNA for site-directed mutagenesis was prepared according to the procedure of Vieira and Messing (1987). Plasmid containing cells in a 5 ml LB culture in early exponential phase were infected with 50  $\mu\text{l}$  of helper phage R408 ( $10^{11}$ - $10^{12}$  PFU per ml) (in presence of 50  $\mu\text{l}$  1 M  $\text{MgSO}_4$ ) and grown overnight. 1.5 ml of overnight grown culture was centrifuged in order to remove the cells and debris. A solution of 300  $\mu\text{l}$  of 1.5 M NaCl, 20% PEG 6000 was added per ml of medium supernatant and mixed by inversion. This mixture was then incubated at room temperature for 15 minutes and centrifuged to pellet the phage particles. The pellet was resuspended in TE buffer on ice and extracted first with an equal volume of buffer-saturated phenol, followed by extraction with an equal volume water-saturated chloroform. Single-stranded DNA was precipitated by addition of an equal volume of 7.5 M ammonium acetate, pH 7.5 and 4 volumes of ice-cold 95% ethanol followed by incubation at  $-20^{\circ}\text{C}$  for 30 minutes. Single stranded DNA was recovered by centrifugation and the pellet was washed once with 95% (v/v) ethanol and two times with 70% (v/v) ethanol. The dried pellet was stored at  $-20^{\circ}\text{C}$  until further use.

#### 2.4.4. Restriction endonuclease digestion of DNA

Restriction digestions were performed at 37°C for 2-5 hours in total volumes of 10  $\mu$ l, containing 1  $\mu$ g RNase, 1  $\mu$ l of 10X appropriate buffer provided by the supplier, ~1-5  $\mu$ g DNA, and 0.5-1  $\mu$ l (50-2,500 Units) of endonuclease.

#### 2.4.5. Agarose gel electrophoresis

Electrophoresis of the restriction endonuclease digested DNA was performed according to Sambrook *et al.*, (1989). Agarose gels containing 1% (w/v) agarose and 0.1  $\mu$ g/ml ethidium bromide were prepared in TAE buffer (40 mM Tris-Acetate and 1 mM EDTA, pH 8.0) and cast in Bio-Rad Mini Sub Cell Plexiglass horizontal electrophoresis trays (6.5 cm x 10 cm). Samples of 10  $\mu$ l volumes were mixed with 2  $\mu$ l Stop buffer (40% [v/v] glycerol, 10 mM EDTA pH 8.0, 0.25% [w/v] bromophenol blue). 1kb DNA ladder or 1 kb plus DNA ladder (Invitrogen Canada Inc.) were used as molecular weight size standards. Electrophoresis was carried out at 40-60 mA constant current in TAE buffer, usually until the bromophenol blue marker dye front had migrated approximately two-thirds of the length of the gel. Following electrophoresis, the DNA bands were visualized with ultraviolet light and recorded in a digitized form using a Gel Doc 1000 image capture system (Bio-Rad).

#### 2.4.6. Ligation

DNA fragments to be ligated were excised from agarose gels and purified using the Ultraclean<sup>TM</sup> 15 DNA purification kit (Bio/Can Scientific Inc.) according to the instructions supplied by the manufacturer. Ligation of insert DNA into vector was carried

out according to the procedure of Sambrook *et al.* (1989). Purified DNA was mixed in a ratio of 2-3 of insert to vector in 10  $\mu$ l volumes, containing 1 unit of T4 DNA ligase (Invitrogen Canada Inc.), and the manufacturer's supplied buffer at the appropriate concentration. Ligation mixtures were incubated overnight at 15 °C. A mixture without the insert DNA added was used as control.

#### **2.4.7. Transformation**

Transformation of *E. coli* cells with the various plasmids was achieved according to Chung *et al.* (1989). 5 ml LB cultures of cells grown to exponential phase (2-4 hours) were harvested by centrifugation and made competent by resuspension in 500  $\mu$ l ice-cold 0.1 M  $\text{CaCl}_2$  for at least 30 minutes on ice. 2-10  $\mu$ g DNA was usually added to 100  $\mu$ l of this cell suspension, followed by a further 30-minute incubation on ice, and a 90 second heat shock at 42 °C. 0.9 ml LB medium was then added to the cell suspension and incubated at 37 °C for 1 hour without aeration. The mixture was either spread, or (in the case of ligation mixture transformations) mixed with 3 ml molten (50°C) R-Top agar (0.125 g yeast extract, 1.25 g tryptone, 1 g NaCl, 1 g agar per 125 ml volume with 0.25 ml 1 M  $\text{CaCl}_2$  and 0.42 ml 30% glucose sterile solutions added after autoclaving) and poured onto ampicillin-containing LB plates.

#### **2.4.8. DNA sequencing**

Sequencing of DNA was performed according to the method of Sanger *et al.* (1977). Sequencing was carried out manually with double stranded DNA templates using the primers shown in Table 2.2. For preparation of double stranded DNA template, 5  $\mu$ g



plasmid DNA was resuspended and denatured in a 40  $\mu$ l volume of 2 M NaOH freshly prepared. This mixture was incubated for 10 minutes at 37 °C, and reprecipitated by addition of 10  $\mu$ l 3M sodium acetate, pH 4.8 and 140  $\mu$ l ice-cold 95% ethanol. Following incubation at -20°C for 30 minutes, the DNA pellet was recovered by centrifugation, washed once with 1 ml 95% ice-cold ethanol, and once with 200  $\mu$ l 70% ice-cold ethanol, and then evaporated to dryness under vacuum in a desiccator. Annealing and sequencing reactions were carried out using a T7 Sequencing Kit (USB Corporation, USA) according to the manufacturer's specifications and using 10  $\mu$ Ci [ $\alpha$ -<sup>35</sup>S] dATP (Amersham Biosciences). Reaction mixtures were separated and resolved on 8% (w/v) polyacrylamide vertical slab gels containing 7 M urea, 0.13 M Tris, 0.13 M boric acid, and 10 mM EDTA. Electrophoresis was carried out using 18-24 mA constant current in TBE buffer (90 mM Tris , 89mM borate, 2.2 mM EDTA) for 1.5-4 hours as required. Gels were mounted on 3 mm paper (Whatman), covered with clear plastic film, and dried at 80°C for about 1 hour on a slab gel drier vacuum (Savant). Dried gels were exposed to X-ray film (Kodak X-OMAT AR) in order to visualize and record the DNA bands.

## **2.5. Purification of BpKatG and its variants**

For small scale crude extracts used in determination of relative levels of protein expression, as well as catalase activity, plasmid containing cells were grown in 30 ml of LB medium in 125 ml shake flasks at 28°C and 37°C for 16-20 hours. Whole cell cultures were assayed for catalase activity and expression profile by electrophoresis on sodium dodecyl sulfate polyacrylamide gels (SDS-PAGE).

For large scale preparations of BpKatG and its variant proteins, UM262 cells over expressing the desired protein from the appropriate plasmid borne genes were grown in 4-6 liters of LB media, in 2 liter shake flasks (500 ml LB per flask) supplemented with 100  $\mu\text{g/ml}$  of ampicillin and 40  $\mu\text{g/ml}$  hemin (Sigma), for 16-20 hours, at either 28°C or 37°C with good aeration. Isolation of BpKatG and its variant proteins were done according to the procedure of Loewen and Switala (1986) with modifications. All isolation and purification steps were carried out at 4°C. Cells were harvested from the growth media by centrifugation and the cell pellet was kept at -60°C overnight. The cell pellet was then resuspended in about 150-250 ml of potassium phosphate 50 mM, pH 7.0 containing 5 mM EDTA. The cells were disrupted by a single pass through a French pressure cell press at 20,000 psi. Unbroken cells and debris were removed by centrifugation, yielding the crude extract, to which was added streptomycin sulfate to a final concentration of 2.5% (w/v). The resulting precipitates were removed by centrifugation and discarded. Solid  $(\text{NH}_4)_2\text{SO}_4$  was then added in appropriate amounts with gentle stirring, to achieve the required concentration followed by centrifugation, to precipitate the desired protein. BpKatG and its variants were found to precipitate in  $(\text{NH}_4)_2\text{SO}_4$  at 40-45% saturation. Pellets from the  $(\text{NH}_4)_2\text{SO}_4$  precipitations were resuspended in 10-20 ml of potassium phosphate 50 mM, pH 7.0. The presence of the desired protein in the pellets was confirmed by assays for catalytic activity and visualization on SDS gels. Resuspensions were centrifuged to remove any remaining precipitates, and dialyzed overnight using a 12,000-14,000 molecular weight cutoff membrane, against 2 liters of potassium phosphate 50 mM, pH 7.0 overnight.

The dialyzed resuspensions were centrifuged and loaded onto a 2.5 cm x 23 cm column of DEAE-cellulose A-500 (Cellufine, Amicon) equilibrated with potassium phosphate 50 mM, pH 7.0. The column was washed with potassium phosphate 50 mM, pH 7.0 until the  $A_{280}$  of the eluting solution was below 0.05. The protein of interest was then eluted with a 0-0.4M NaCl linear gradient in potassium phosphate 50 mM, pH 7.0, usually in a total volume of 1 liter. Eighty-drop fractions of the eluted proteins from the column were collected throughout. Purity of the recovered column fractions was based on  $A_{280}$  and catalase activity elution profiles or on  $A_{280}$  and  $A_{407}$  elution profiles (in case of mutations that had low or no catalase activity). Selected fractions were pooled and concentrated under nitrogen in a stirred pressure cell (Model 8050, Amicon) using a YM-30 (Amicon) membrane, to volumes of between 5-10 ml. The concentrated protein sample was then dialyzed against approximately 1 liter of potassium phosphate 50 mM, pH 7.0 overnight. The concentrated, dialyzed proteins were checked for purity using catalase activity, the  $A_{407/280}$  (heme/protein) ratios and visualization using SDS-PAGE. The protein was then loaded on to a 2.5 x 15 cm hydroxyapatite column (Bio-Rad) equilibrated with potassium phosphate 5 mM, pH 7.0. The protein was eluted with potassium phosphate 5-200 mM, pH 7.0, usually in a final volume of 500 ml. Fifty-drop fractions of the eluted proteins from the column were collected throughout. Selected fractions were then pooled and concentrated as before. The purified protein samples were aliquoted into eppendorf tubes in 0.5 ml volumes and stored frozen at  $-60^{\circ}\text{C}$  until use.

## **2.6. Sodium dodecyl sulfate-polyacrylamide gel electrophoresis (SDS-PAGE)**

Denaturing SDS-PAGE was carried out according to Weber et al., (1972).

Discontinuous 4% stacking and 8% separating polyacrylamide gels were cast as vertical slabs of dimensions 10 x 10 cm and 0.5 mm thickness (mini gels). Samples loaded onto the mini gels usually contained about 10-20  $\mu\text{g}$  protein for crude extracts or 2-5  $\mu\text{g}$  protein for purified protein. Protein samples were mixed with equal volumes of reducing denaturing sample buffer (3.4 mg/ml  $\text{NaH}_2\text{PO}_4$ , 10.2 mg/ml  $\text{Na}_2\text{HPO}_4$ , 10 mg/ml SDS, 0.13 mM 2-mercaptoethanol, 0.36 g/ml urea and 0.15% bromophenol blue) and boiled for 3 minutes before loading onto the gels. Samples were run with 150 V constant voltage in a vertical BIO-RAD Mini-Protean II electrophoresis system, using a running buffer containing 14 g glycine, 3 g Tris base, and 1 g SDS per liter. Gels were stained in a solution containing 0.5 g/l Coomassie Brilliant Blue R-250, 30% ethanol and 10% acetic acid for one hour, and destained with repeated changes of destaining solution containing 15% methanol and 7% acetic acid, until the background was clear. Finally the gels were soaked in the last destaining solution containing 7% acetic acid and 1% glycerol for 30 minutes. Gels were then mounted on 3 mm (Whatman) paper, covered with a clear plastic film, and dried at 80°C for 1 hour on a slab gel drier under vacuum (Savant).

## **2.7. Enzymatic assays and protein quantitation**

Catalase activity was determined by the method of Rørth and Jensen (1967) in a Gilson oxygraph equipped with a Clark electrode. One unit of catalase is defined as the amount of enzyme that decomposes 1  $\mu\text{mol}$  of  $\text{H}_2\text{O}_2$  in 1 minute in 60 mM  $\text{H}_2\text{O}_2$  solution

at pH 7 and 37°C. 1.8 ml of 50 mM potassium phosphate buffer, pH 7 was added to the reactor chamber followed by addition of 50  $\mu$ l of H<sub>2</sub>O<sub>2</sub> solution to a final concentration of 60 mM, incubated for 0.5-1.0 minute at 37°C, then appropriately diluted enzyme samples or cell cultures were added. Catalase activity as units/ml was determined from the slope of oxygen evolution. Specific catalase activity was expressed as units $\cdot$ ml<sup>-1</sup> $\cdot$ mg<sup>-1</sup> purified protein. Specific catalase activity in whole cells (units/mg dry cell weight) was determined by converting the cell turbidity values at 600 nm to Klett values. Specific activity was always determined as the average of three or more determinations.

Peroxidase activity was determined spectrophotometrically by the o-dianisidine method described in the Worthington Enzyme Catalogue (Worthing Chemical Co., 1969). Assays were carried out at room temperature in 1 ml final assay volumes containing 1 mM H<sub>2</sub>O<sub>2</sub>, 0.34 mM o-dianisidine in 50 mM sodium acetate buffer pH 4.5. Aliquots (1-5  $\mu$ l) of the appropriately diluted enzymes were added to initiate reaction. Peroxidase activity was determined by the  $\Delta A_{460}$ /min average over periods of 2 min and expressed as units $\cdot$ mg<sup>-1</sup> $\cdot$ ml<sup>-1</sup> purified protein calculated as: ( $\Delta A_{460}$ /min)/(11.3 x mg enzyme/ml reaction mixture), using a molar extinction coefficient at A<sub>460</sub> nm for o-dianisidine product of 11,300 M<sup>-1</sup>cm<sup>-1</sup>. Peroxidase activity was also determined spectrophotometrically by the 2,2'-azinobis {3-ethylbenzothiazolinesulfonic acid} (ABTS) method (Smith *et al.*, 1990) with minor modifications. Assays were carried out at room temperature in 1 ml final assay volumes containing 2.5 mM H<sub>2</sub>O<sub>2</sub>, 0.4 mM ABTS in 50 mM sodium acetate buffer pH 4.5. Aliquots (1-5  $\mu$ l) of the appropriately diluted enzymes were added to initiate reaction. Peroxidase activity was determined by the  $\Delta A_{405}$ /min average over periods of 2 min and expressed as units $\cdot$ mg<sup>-1</sup> $\cdot$ ml<sup>-1</sup> purified

protein calculated as:  $(\Delta A_{405}/\text{min})/(36.8 \times \text{mg enzyme/ml reaction mixture})$ , using a molar extinction coefficient of ABTS product at  $A_{405}$  nm of  $36,800 \text{ M}^{-1}\text{cm}^{-1}$ . One unit of peroxidase activity is defined as the amount that decomposes  $1 \mu\text{mol}$  of electron donor (ABTS or o-dianisidine) in 1 minute at pH 4.5 and room temperature.

Isoniazid (INH) hydrazinolysis by BpKatG was determined spectrophotometrically at 560 nm by monitoring the reduction of nitroblue tetrazolium (NBT) to a monoformazan dye ( $\epsilon = 15,000 \text{ M}^{-1}\text{cm}^{-1}$ ) by enzymatically oxidized radical species of isoniazid. Assays were carried out in 1 ml final volumes containing 10 mM INH and 200  $\mu\text{M}$  NBT in 50 mM tris buffer, pH 8, at room temperature. Aliquots (1-5  $\mu\text{l}$ ) of the appropriately diluted enzymes were added to initiate the reaction. Nicotinamide adenine dinucleotide (NADH) oxidase activity was determined spectrophotometrically at 560 nm by monitoring the reduction of nitroblue tetrazolium (NBT) to a monoformazan dye by enzymatically oxidized radical species of NADH. Assays were carried out in 1 ml final volumes containing 250  $\mu\text{M}$  NADH and 200  $\mu\text{M}$  NBT in 50 mM tris buffer, pH 8, at room temperature. Aliquots (1-5  $\mu\text{l}$ ) of the appropriately diluted enzymes were added to initiate the reaction. INH hydrazinolysis activity was determined by the  $\Delta A_{560}/\text{min}$  average over periods of 10 min. NADH oxidase activity was determined by the  $\Delta A_{560}/\text{min}$  average over periods of 5 min. INH hydrazinolysis and NADH oxidase activities were expressed as  $\text{units} \cdot \text{mg}^{-1} \cdot \text{ml}^{-1}$  purified protein by using a molar extinction coefficient of  $15,000 \text{ M}^{-1} \cdot \text{cm}^{-1}$  for the monoformazan product from the reduction of NBT. One unit of INH hydrazinolysis and NADH activities are defined as the amount that produces 1 nmol of free radical in 1 minute in a 10 mM INH or 250  $\mu\text{M}$  NADH solution at pH 8.0 and room temperature.

NADH oxidase activity was also directly determined spectrophotometrically at 340 nm by monitoring the rate of NADH disappearance. Assays were carried out in 1 ml final volumes containing 250  $\mu$ M NADH in 50 mM tris buffer, pH 8, at room temperature. Aliquots (1-5  $\mu$ l) of the appropriately diluted enzymes were added to initiate the reaction. NADH oxidase activity was determined by the  $\Delta A_{340}/\text{min}$  average over periods of 5 min. NADH oxidase activities were expressed as  $\text{units} \cdot \text{mg}^{-1} \cdot \text{ml}^{-1}$  purified protein, using a molar extinction coefficient of  $6,300 \text{ M}^{-1} \cdot \text{cm}^{-1}$  for NADH. One unit of NADH activity is defined as the amount that decomposes 1 nmol of NADH in 1 minute in a solution of 250  $\mu$ M NADH at pH 8.0 and room temperature.

Protein concentration (mg/ml) was estimated spectrophotometrically based on  $A_{280}$  calculated as:  $(A_{280} \times 79198) / 138870$ , where the molar extinction coefficient of BpKatG is 138870 based on amino acid composition and the molecular weight of BpKatG is 79198. Specific activities were always determined as the average of a minimum of three or more individual determinations.

## 2.8. Absorption spectrophotometry

Absorption spectra, time courses, and peroxidatic assays were performed using a Pharmacia Ultrospec 4000 Spectrophotometer, a Milton Roy MR300 Spectrophotometer or Ultrospec 3100 pro. All experiments were performed at ambient temperature in 1 ml quartz, semimicro cuvettes. Proteins were diluted in 50 mM potassium phosphate buffer, pH 7.0 unless otherwise stated, and the same buffer was used as a reference. For the ABTS and o-dianisidine peroxidation assays, proteins were diluted in 50 mM sodium

acetate buffer, pH 4.5 and the same buffer was used as a reference. For preparation of spectral and time course plots, data collected were transferred to Sigma Plot software.

## **2.9. Effects of inhibitors**

The effects of classical heme inhibitors, KCN and  $\text{NaN}_3$  on catalase activity of wild type BpKatG and its variants were studied. For assays of catalase activity in presence of different concentrations of KCN and  $\text{NaN}_3$ , the enzyme was incubated for 1 minute in the reaction mixture containing one of the above compounds prior to initiation of the reaction by addition of  $\text{H}_2\text{O}_2$ .



### 3. RESULTS

#### 3.1. Introduction

Based on the crystal structures of catalase-peroxidases from *Haloarcula marismortui* (Yamada *et al.*, 2001) and *Burkholderia pseudomallei* (BpKatG) (Carpena *et al.*, 2003), four residues are located in the distal side active site of the enzyme, arginine, histidine, tryptophan and aspartate (residues 108, 112, 111 and 141 respectively in BpKatG), which are highly conserved among known catalase-peroxidases. Previous studies using the catalase-peroxidase from *Escherichia coli* (EcKatG) suggested that the tryptophan, arginine and histidine are indeed active site residues because they are important for enzyme catalysis (Hillar *et al.*, 2000). Similarly, the aspartate in the catalase-peroxidase from the cyanobacterium *Synechococcus* (SyKatG) is critical for catalytic activity, but not for peroxidatic activity (Jakopitsch *et al.*, 2003). The goal of this study was to confirm the catalytic and structural roles of the conserved arginine, histidine and aspartate in BpKatG. The tryptophan residue is considered elsewhere.

#### 3.2. Characterization of BpKatG variants

The BpKatG variants, R108A, R108K, H112A, H112N, D141A, D141N and D141E, were purified as outlined in Table 3.1 and described in Materials and Methods. The wildtype and variant proteins were analyzed by SDS-PAGE (Figure 3.2a) revealing similar electrophoretic mobilities and a predominant band with an apparent molecular mass of about 79 kDa. The larger band at approximately 160 kDa is probably crosslinked dimer which is not reduced by either  $\beta$ -mercaptoethanol or dithiothreitol added to the

sample buffer. If smaller amounts of proteins (~1  $\mu$ g) were analyzed by SDS-PAGE, the presence of a double band becomes obvious in place of the single band for the Arg108 and His 112 variants (Figure 3.2b). This is probably a result of incomplete formation of the covalent structure linking Trp111, Tyr238 and Met264 (Figure 3.1).

Figure 3.3 compares the absorption spectra of the variants with that of the wild type BpKatG. Table 3.2 summarizes the positions of absorption maxima, heme/protein ratio ( $A_{407/280}$ ) and heme/subunit ratio. The Sorêt band is within one nm of 407 nm for all variants except R108K where it is red shifted by 8 nm to 415 nm. The H112A and H112N variants also show a small shoulder at 375 nm. The spectra in 500-700 nm region were also the same for all variants except R108K where the shoulder at 640 nm is decreased (Figure 3.3). Shifts in the charge transfer bands between 500 and 700 nm are generally indicators of changes in the hydrogen bond network in the vicinity of the heme. All variants and wild type show similar  $A_{407/280}$  ratio between 0.48-0.65 suggesting 0.67 to 0.90 heme per subunit.

### 3.3. Biochemical characterization of BpKatG variants

Table 3.3 summarizes the catalase and peroxidase activities of the BpKatG variants. The catalase specific activities of all of the variants are reduced to 0.1 - 87% of the wild type BpKatG activity. Two different organic electron donors (ABTS and o-dianisidine) were evaluated as substrates for the peroxidatic reaction. All of the variants exhibit reduced peroxidase activity in comparison to the wild type ranging 1-2% to 83% of wild type activity.

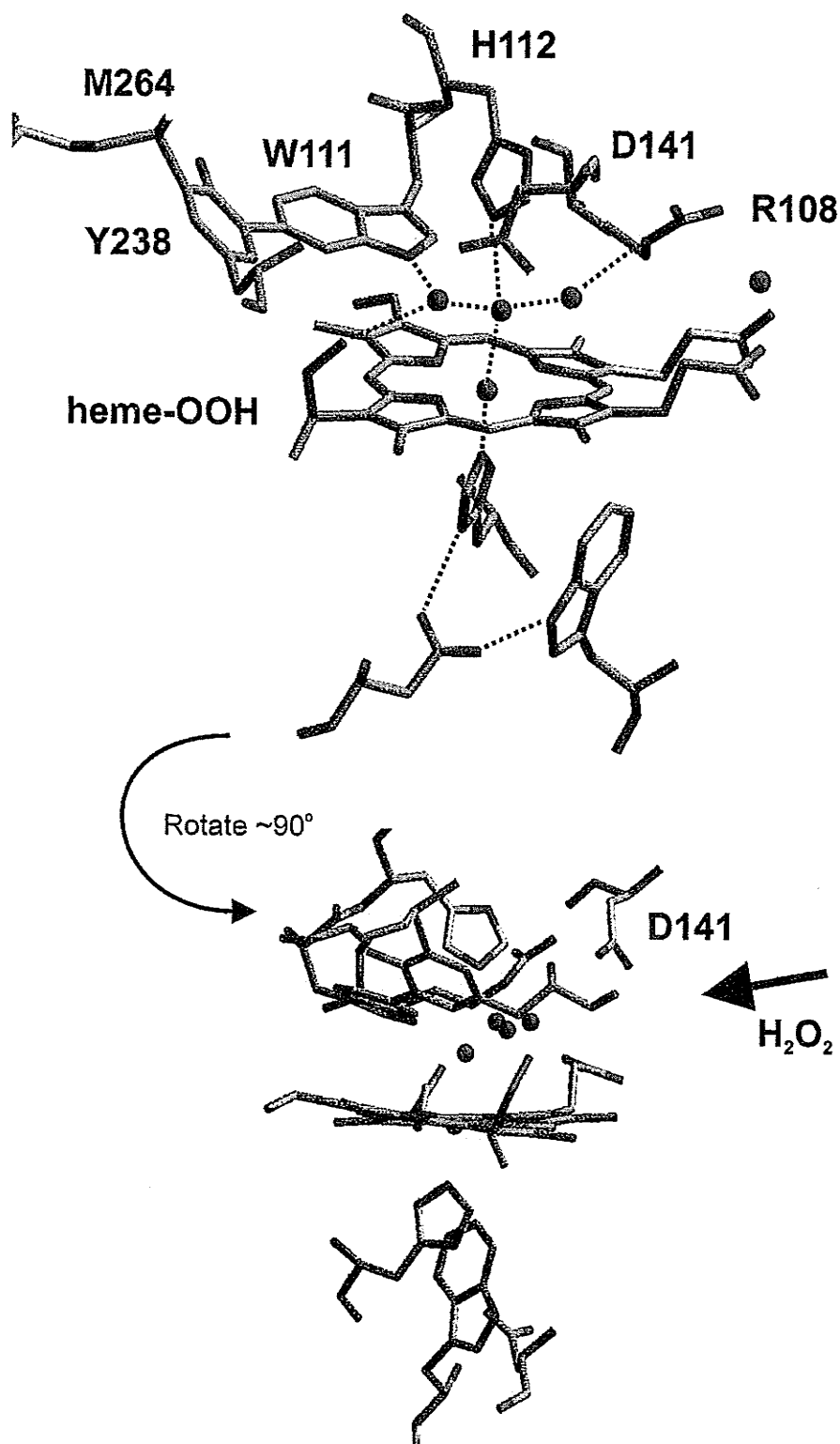


**Figure 3.1.** Two views of residues in the active site of BpKatG related by a 90° rotation. Top view shows Arg108, His112 and Asp141 on the distal side of the heme and the covalent structure linking Trp111, Tyr238 and Met264. Bottom view shows the location of Asp141 close to the substrate access channel.

**Table 3.1.** Purification of wild type BpKatG from the *Escherichia coli* strain UM262 harbouring plasmid encoded *katG* of *Burkholderia pseudomallei*.

Purification Step	Total Protein (mg)	Total catalase activity (units x 10 <sup>3</sup> )	Specific catalase activity (units/mg)	Recovery (%)	Purification (fold)
Crude extract	7332	774	106	100	1
(NH <sub>4</sub> ) <sub>2</sub> SO <sub>4</sub> precipitation	409	581	1421	75	14
Anion exchange (DEAE-A-500)	66	250	3780	32	38

R108A, R108K, H112A, H112N, D141A, D141N and D141E variants were also purified using the above protocol.

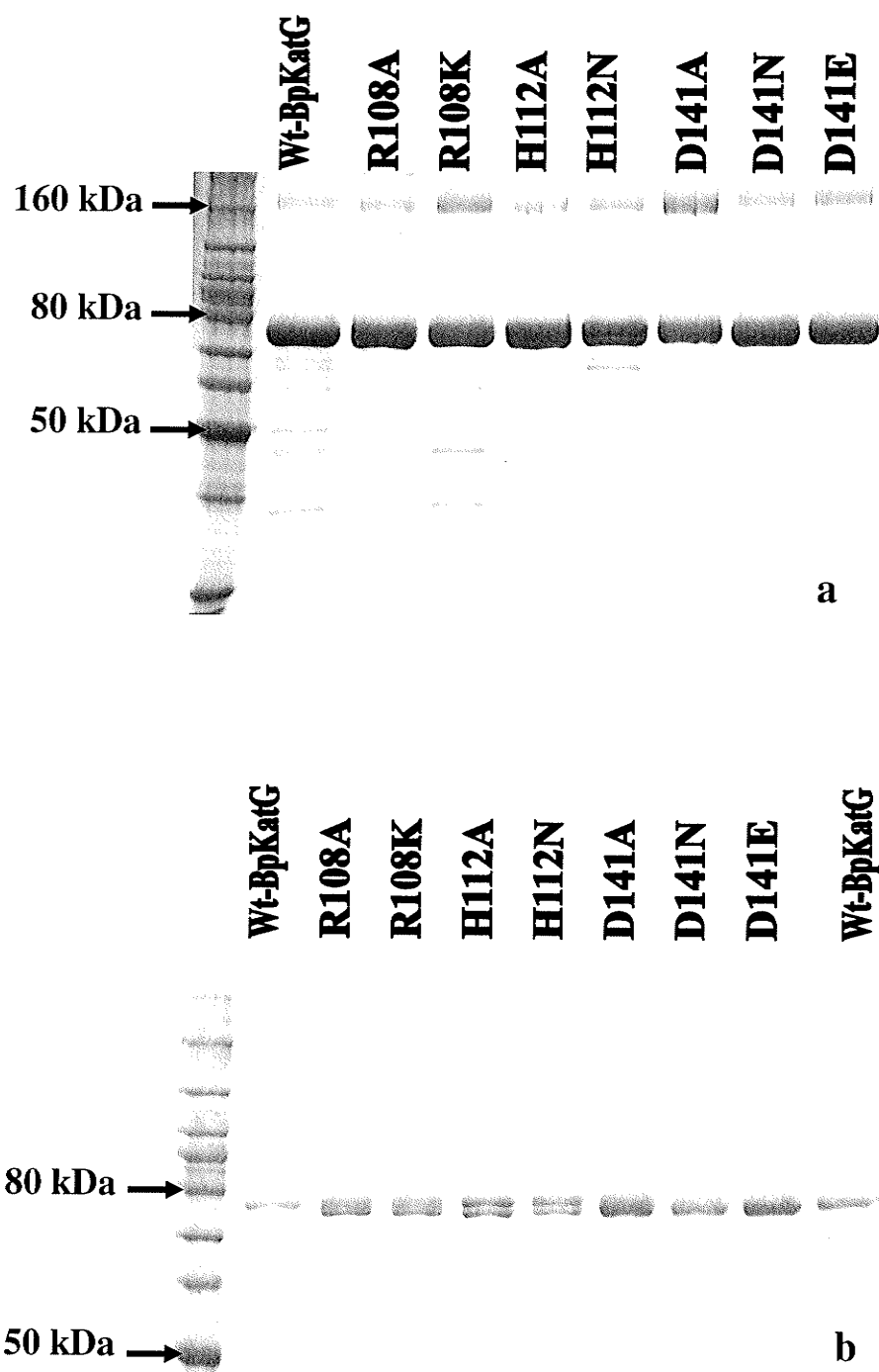


**Figure 3.2.** SDS-polyacrylamide gel electrophoretic analysis of purified wild type BpKatG and its variants.

- a) Approximately 2.5  $\mu$ g of samples were run on the gel.
- b) Approximately 1  $\mu$ g of samples were run on the gel.

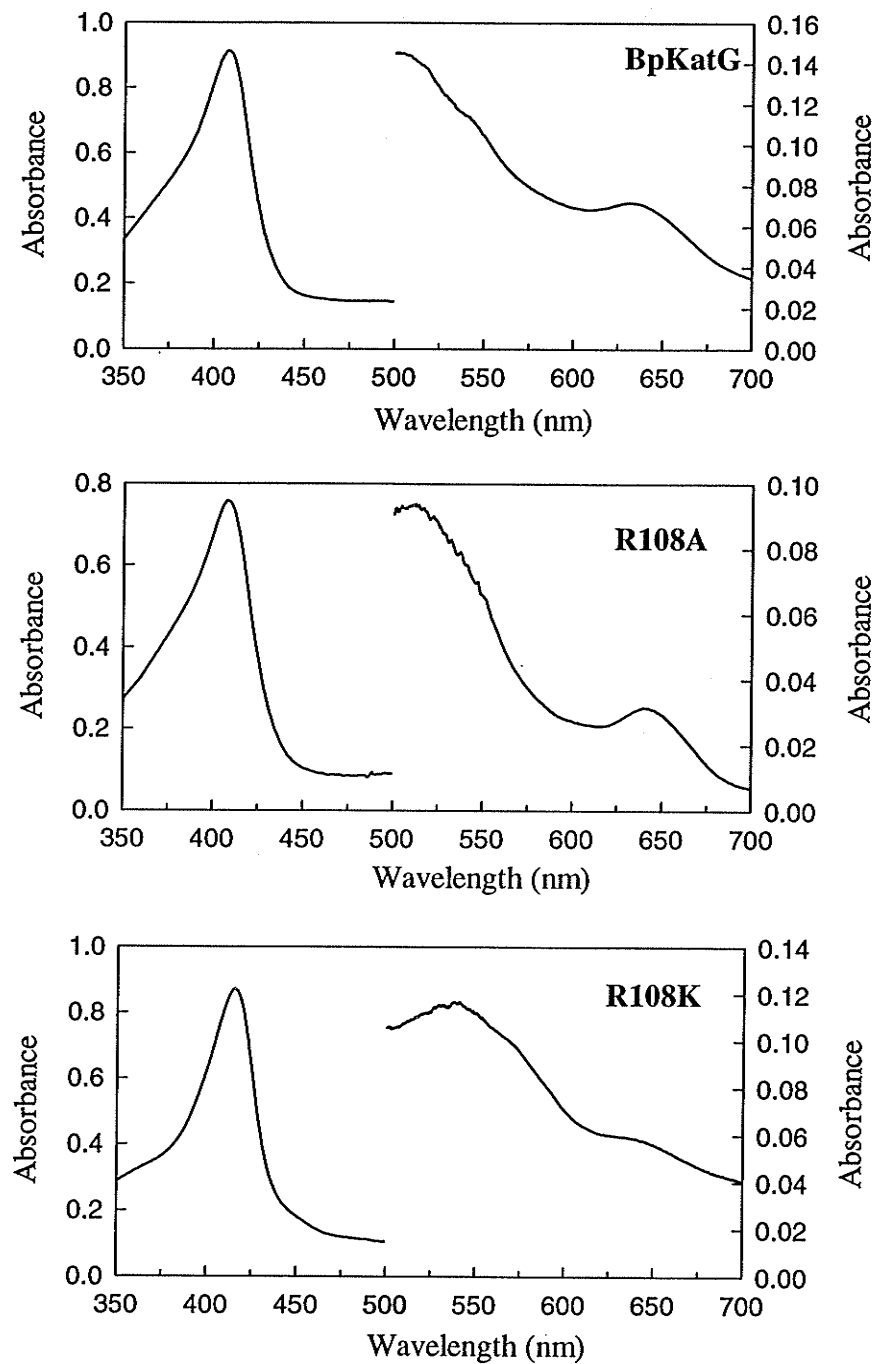


**Figure 3.3.** Absorption spectra of wild-type BpKatG and its variants. Left axis scales apply to the 350-500 nm wavelength range. Right axis scales apply to the 500-700 nm wavelength range.

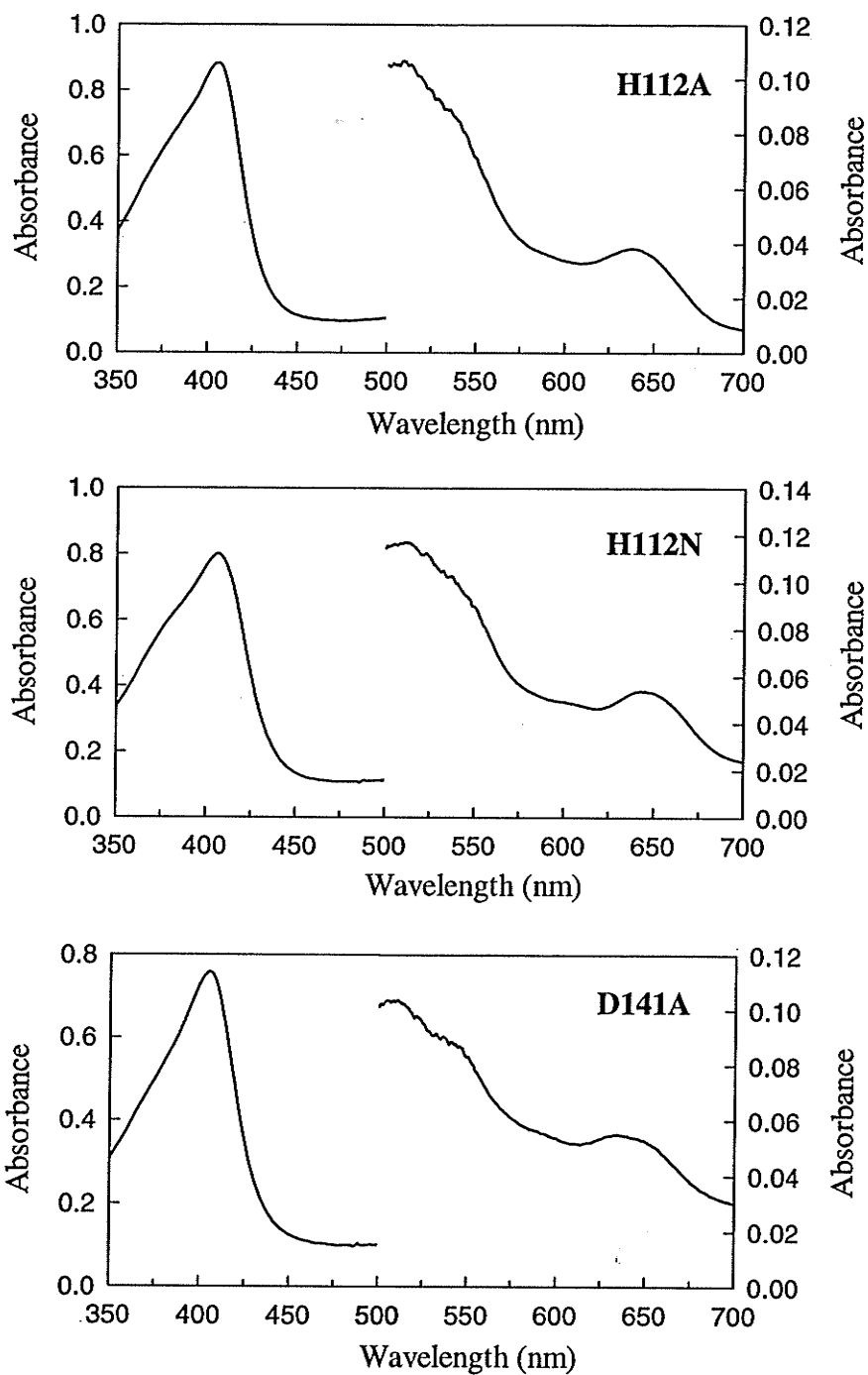
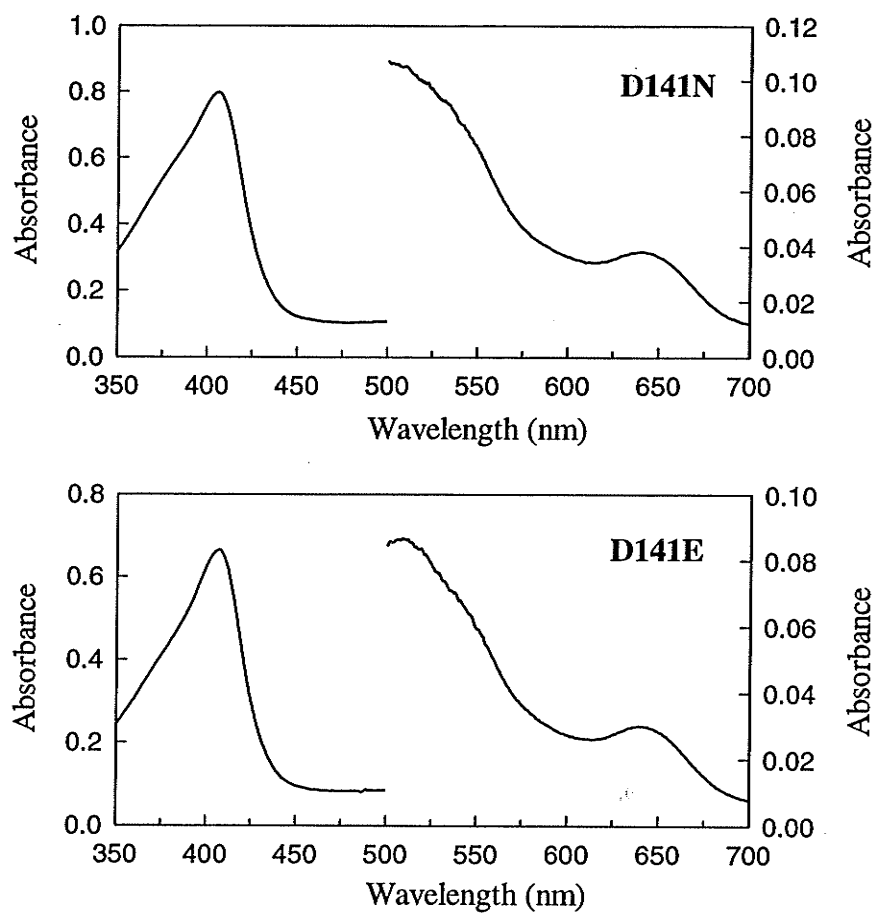


Figure 3.3. (continued)



**Figure 3.3. (continued)**



**Table 3.2.** Summary of observed optical absorbance maxima,  $A_{407/280}$  ratio and heme/subunit ratio for purified BpKatG and its variants.

Mutant	Sorêt maximum (nm)	$A_{407/280}$ ratio	Heme/subunit ratio
<b>Wild-type</b>	407	0.61	0.85
R108A	407	0.58	0.81
R108K	415	0.51	0.71
H112A	406	0.65	0.90
H112N	406	0.48	0.67
D141A	406	0.59	0.82
D141N	406	0.57	0.79
D141E	406	0.55	0.76

BpKatG has recently been shown to catalyze the oxidation of NADH to NAD<sup>+</sup> and the hydrazinolysis of isonicotinic acid hydrazide (INH) (Singh *et al*, 2004). The NADH oxidase activity was assayed directly, following the rate of NADH disappearance spectrophotometrically at 340 nm, and indirectly using NBT (nitroblue tetrazolium) as a radical sensor to follow the superoxide radical formation spectrophotometrically at 560 nm. The INH hydrazinolysis activity was assayed using NBT as a radical sensor to follow the production of isonicotinoyl radical spectrophotometrically at 560 nm. Table 3.4 summarizes the NADH oxidase and INH hydrazinolysis activities of the BpKatG variants. The NADH oxidase activities of the variants are reduced in comparison to that of the wild type BpKatG, most dramatically for the H112A mutant, where there was no detectable activity. Similarly the INH hydrazinolysis activity of the variants are all reduced compared to that of the wild type enzyme.

### 3.4. Kinetic characterization

The effect of [H<sub>2</sub>O<sub>2</sub>] on the rate of catalase reaction of BpKatG and its variants is shown in Figure 3.4. The initial velocities ( $V_i$ ) have been corrected for differing heme content and expressed as micromoles of hydrogen peroxide decomposed per minute per micromole of heme. The effect of [ABTS] on the rate of peroxidase reaction of BpKatG and its variants is shown in Figure 3.5. The initial velocities ( $V_i$ ) have also been corrected for differing heme and expressed as micromoles of ABTS oxidized per minute per micromole of heme. The kinetic constants of the catalase and peroxidase are summarized in Tables 3.5 and 3.6 respectively.

**Table 3.3.** Catalase and peroxidase activities of BpKatG and its variants.

Mutant	Catalase (units/mg) <sup>a</sup>	Peroxidase ABTS (units/mg) <sup>a</sup>	Peroxidase o-dianisidine (units/mg) <sup>a</sup>
<b>Wild-type</b>	3,780 ± 130	6.8 ± 0.4	8.1 ± 0.2
R108A	1,250 ± 110	1.0 ± 0.1	7.5 ± 0.5
R108K	325 ± 20	0.9 ± 0.1	3.6 ± 0.4
H112A	1 ± 0.2	0.1 ± 0.01	0.1 ± 0.01
H112N	2 ± 0.6	0.1 ± 0.01	0.1 ± 0.01
D141A	60 ± 10	5.8 ± 0.4	6.5 ± 0.02
D141N	390 ± 20	5.4 ± 0.5	4.5 ± 0.07
D141E	3,290 ± 40	6.3 ± 0.3	2.5 ± 0.04

<sup>a</sup>(1 unit = 1 μmol/min).

**Table 3.4.** NADH oxidase and INH hydrazinolysis activities of BpKatG and its variants.

Mutant	NADH oxidase (units/mg) <sup>a</sup> at A <sub>340</sub>	NADH oxidase (units/mg) <sup>a</sup> at A <sub>560</sub>	INH Hydrazinolysis (units/mg) <sup>a</sup>
Wild-type	6.9 ± 1.0	7.7 ± 1.2	0.9 ± 0.02
R108A	3.7 ± 0.5	2.2 ± 0.4	0.3 ± 0.01
R108K	2.2 ± 0.3	1.3 ± 0.1	0.3 ± 0.01
H112A	nd <sup>b</sup>	nd <sup>b</sup>	nd <sup>b</sup>
H112N	3.1 ± 0.3	1.3 ± 0.5	0.2 ± 0.06
D141A	2.2 ± 0.2	0.7 ± 0.1	0.5 ± 0.04
D141N	2.8 ± 0.1	1.2 ± 0.3	0.6 ± 0.04
D141E	3.4 ± 0.5	2.8 ± 0.3	0.8 ± 0.03

<sup>a</sup>(1 unit = 1 nmol/min).,

<sup>b</sup>nd : not detectable.

Figures 3.4 and 3.5 show that all of variants follow Michaelis-Menten kinetics except R108A and R108K when analyzed using ABTS.

The data in Table 3.5 show that the  $K_m$  values for  $H_2O_2$  for all of the variants except D141A are higher than the wild type and the  $k_{cat}$  values are all significantly decreased, except for D141E. The catalase  $k_{cat}/K_m$  values of all of the variants are lower than that of the wild type.

The data in Table 3.6 show that the peroxidase  $K_m$  values of all of variants except R108A are significantly lower than the wild type and the  $k_{cat}$  values of all of variants except D141N are significantly decreased, particularly the His112 variants. The peroxidase  $k_{cat}/K_m$  values of the Arg108 and His112 variants are all lower than that of the wild type, but those of Asp141 variants are higher than wild type.

### 3.5. Effect of heme inhibitors on the catalase activity

Figure 3.6 and Figure 3.7 compare the effect of KCN and  $NaN_3$  on the catalase activity of BpKatG and its variants. KCN and  $NaN_3$  are common heme-binding inhibitors used in structure-function studies of heme-containing enzymes. H112A and H112N variants were not tested due to the requirement for extremely large concentrations of enzyme in order to achieve reaction rates high enough to study the effects of inhibitor action. Both KCN and  $NaN_3$  showed similar inhibition patterns for catalase activities of the variants in relation to the wild type, although a much higher  $[NaN_3]$  was required. The R108A variant showed decreased susceptibility to inhibition by both KCN and  $NaN_3$  whereas the R108K variant showed decreased susceptibility to inhibition by KCN, but

slightly more sensitive to  $\text{NaN}_3$ . The D141 variants were more sensitive to KCN but less sensitive to  $\text{NaN}_3$ .

Table 3.7 summarizes protein concentrations present in the reaction mixture and the inhibitor concentrations that cause 50% inhibition of catalase activity. The R108K and R108A variants were less sensitive to KCN than wild type by two and three times respectively. The R108A variant also showed greatly reduced susceptibility to  $\text{NaN}_3$ , whereas R108K did not exhibit any significant changes to inhibition by  $\text{NaN}_3$ . The greatest increase in the sensitivity to KCN was observed for the Asp141 variants. The data showed that less than 10% of [KCN] needed for wild type caused 50% inhibition of the Asp141 variants. By contrast, 2 times more  $[\text{NaN}_3]$  was required to inhibit the Asp141 variants compared to wild type.

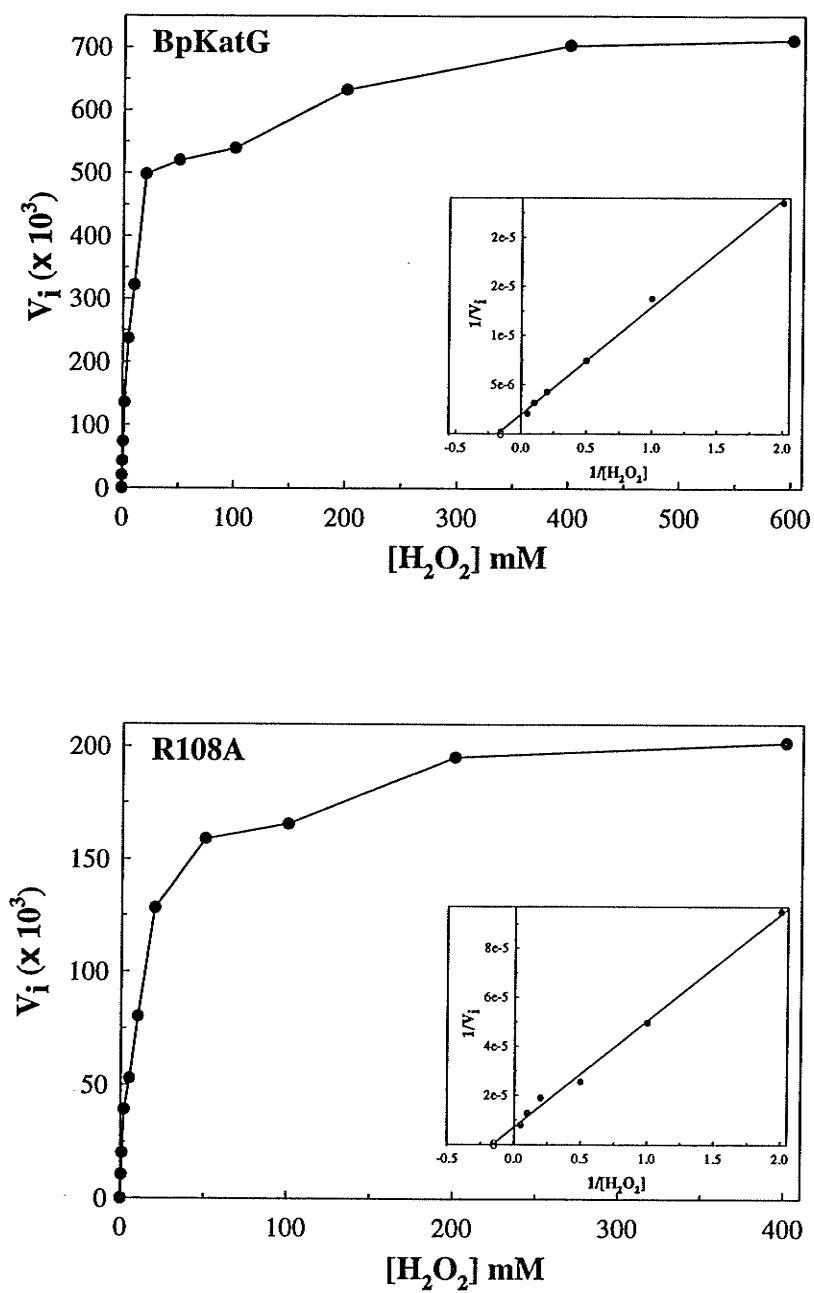


**Figure 3.4.** Effect of  $H_2O_2$  concentration on the initial catalytic velocities ( $V_i$ ) of wild type BpKatG and its variants. Outer panels: Michaelis-Menten (primary plots); Inset panels: Lineweaver-Burk plots (double reciprocal) plots.  
 $V_i = \mu\text{mole of } H_2O_2 \text{ decomposed min}^{-1} \mu\text{mole heme}^{-1}$

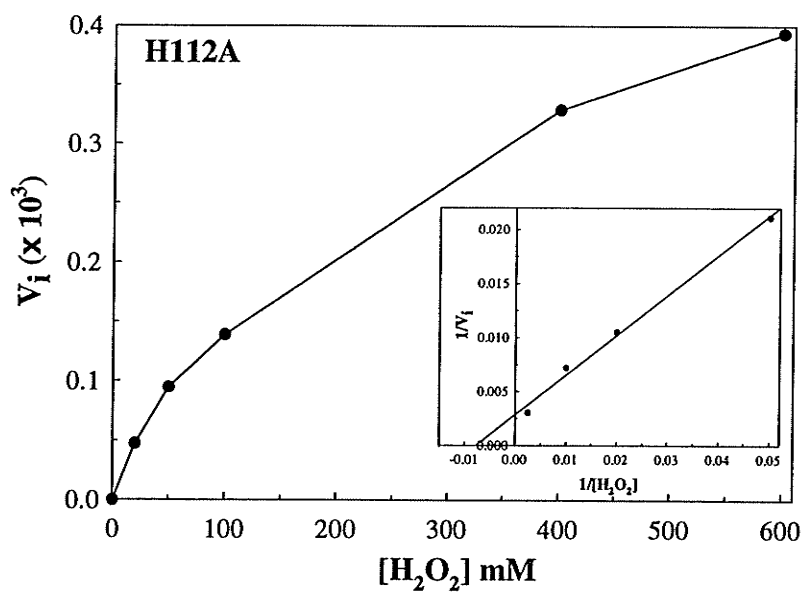
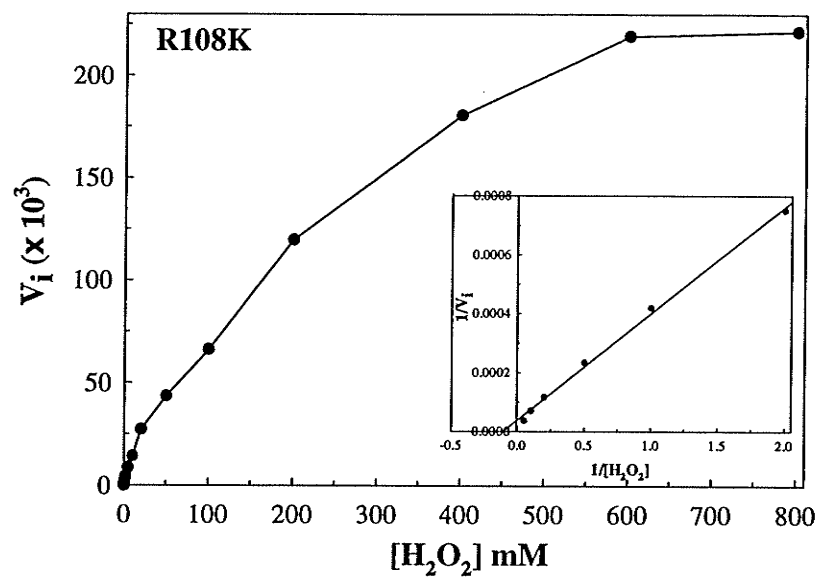


Figure 3.4. (continued)



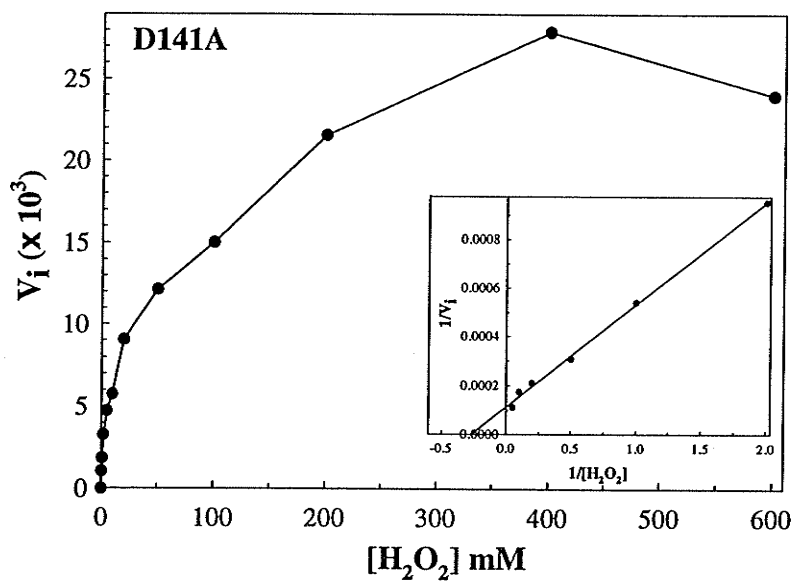
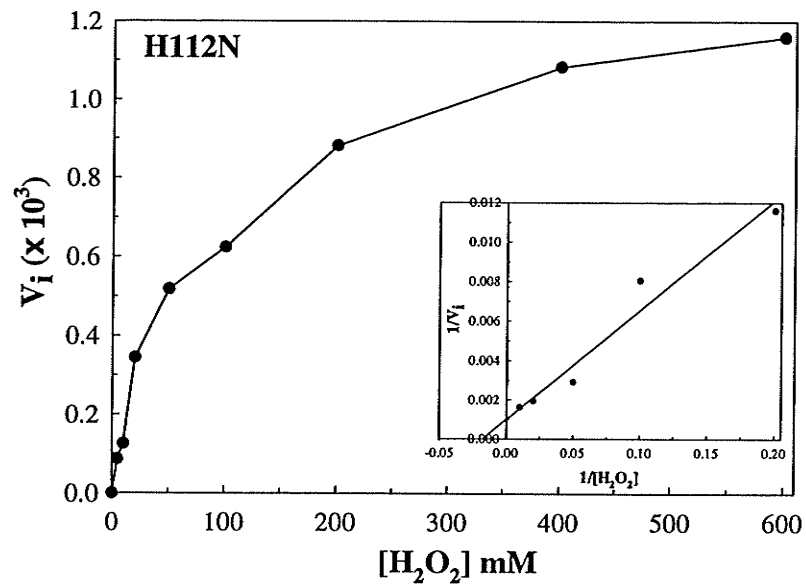


Figure 3.4. (continued)

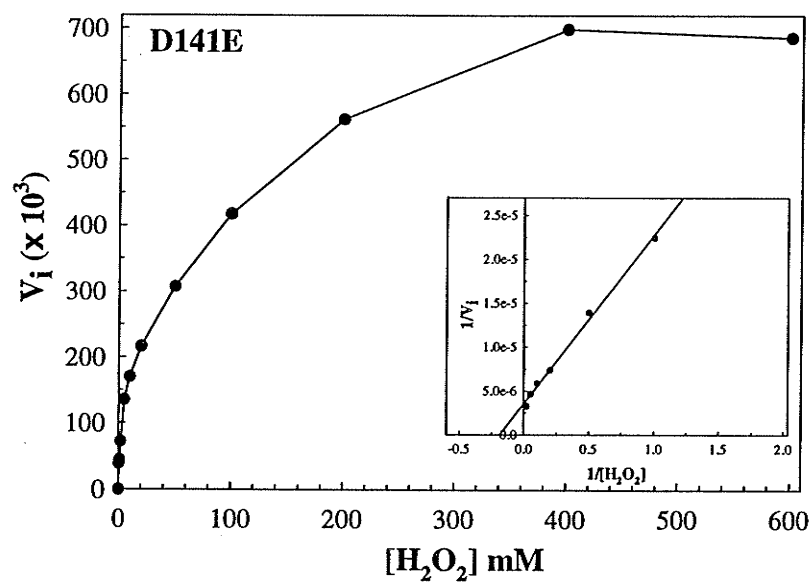
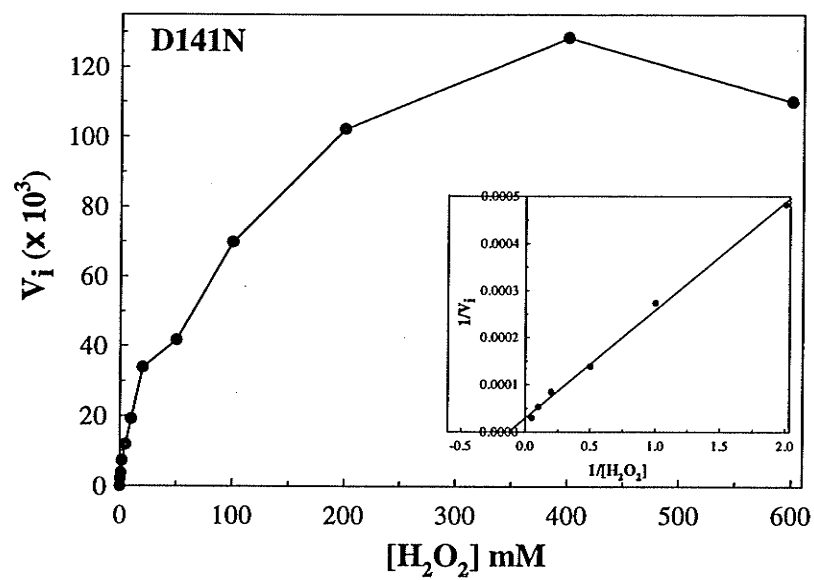
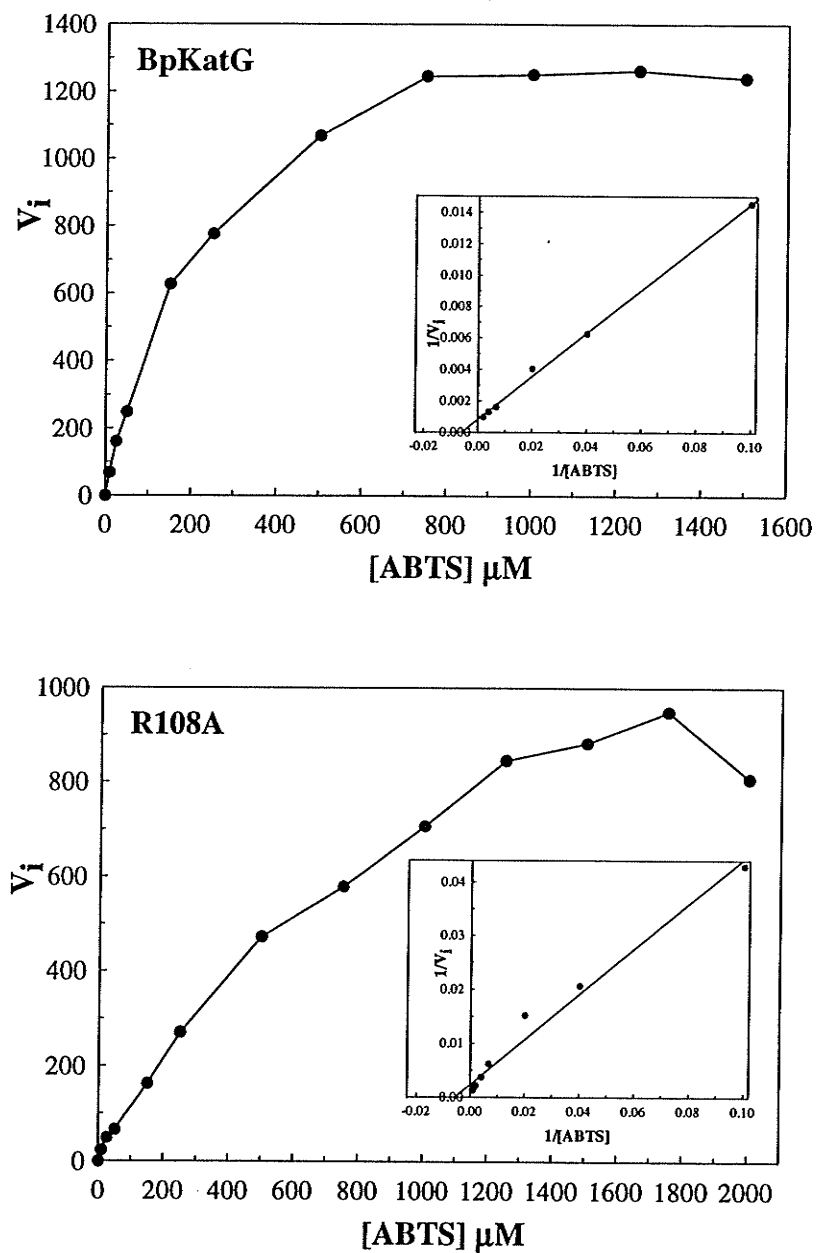


Figure 3.4. (continued)

**Table 3.5.** Comparison of the observed catalytic kinetic parameters of purified wildtype BpKatG and its variants, using H<sub>2</sub>O<sub>2</sub> as substrate.

Variant	$V_{\max}^a$ ( $\times 10^3$ )	$K_m$ (mM)	$k_{\text{cat}}$ (s <sup>-1</sup> )	$k_{\text{cat}}/K_m$ (M <sup>-1</sup> s <sup>-1</sup> )
Wt-BpKatG	556 ± 14	5.9 ± 0.1	9,267 ± 233	1.6 × 10 <sup>6</sup>
R108A	143 ± 6	6.3 ± 0.2	2,383 ± 100	3.8 × 10 <sup>5</sup>
R108K	29 ± 0.9	9.5 ± 0.2	483 ± 15	5.1 × 10 <sup>4</sup>
H112A	0.4 ± 0.01	128 ± 2.6	5.8 ± 0.2	4.6 × 10
H112N	1.0 ± 0.02	57 ± 0.9	17 ± 0.3	3.0 × 10 <sup>2</sup>
D141A	10 ± 0.6	4.7 ± 0.3	167 ± 10	3.6 × 10 <sup>4</sup>
D141N	33 ± 1.6	8.0 ± 0.2	556 ± 2.7	6.9 × 10 <sup>4</sup>
D141E	360 ± 2	6.9 ± 0.8	6,000 ± 33	8.7 × 10 <sup>5</sup>

<sup>a</sup>  $V_{\max}$  is expressed as  $\mu\text{moles of H}_2\text{O}_2 \text{ decomposed min}^{-1} \mu\text{mole heme}^{-1}$



**Figure 3.5.** Effect of ABTS concentration on the initial peroxidatic velocities ( $V_i$ ) of wild type BpKatG and its variants. Outer panels: Michaelis-Menten (primary plots); Inset panels: Lineweaver-Burk (double reciprocal) plots.  
 $V_i = \mu\text{moles of ABTS oxidized min}^{-1} \mu\text{mole of heme}^{-1}$

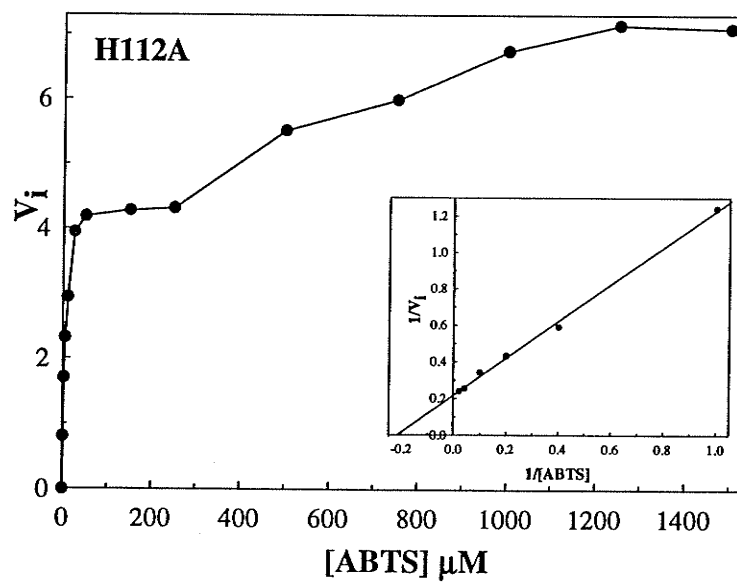
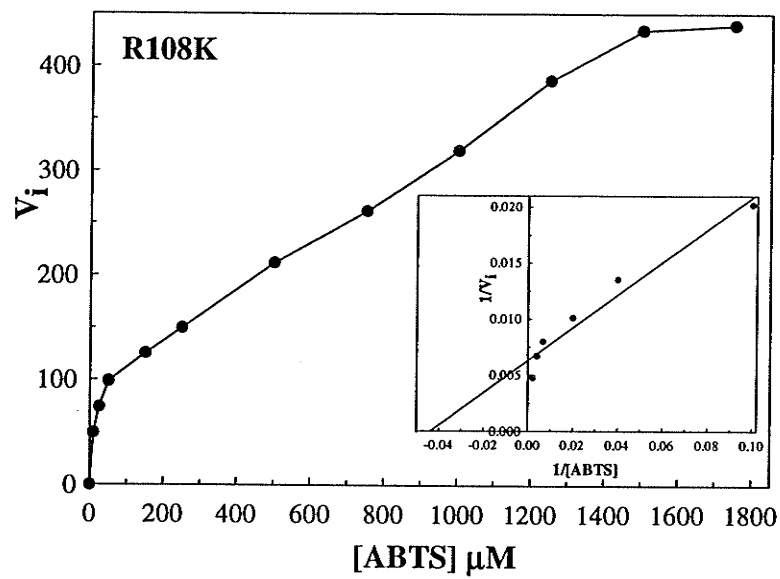


Figure 3.5. (continued)

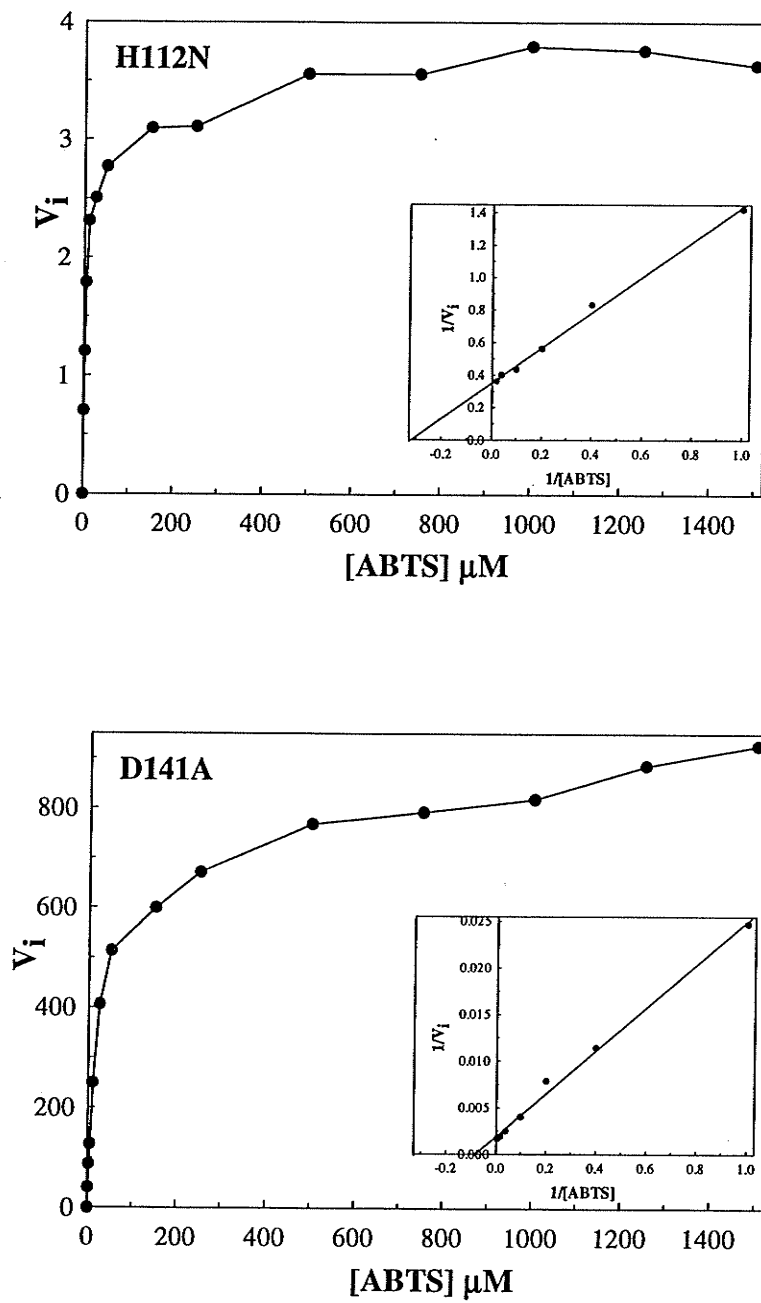


Figure 3.5. (continued)

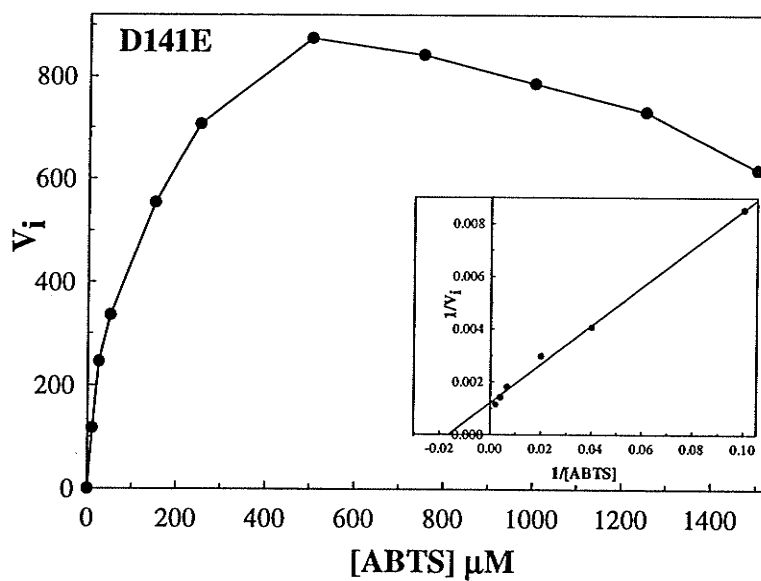
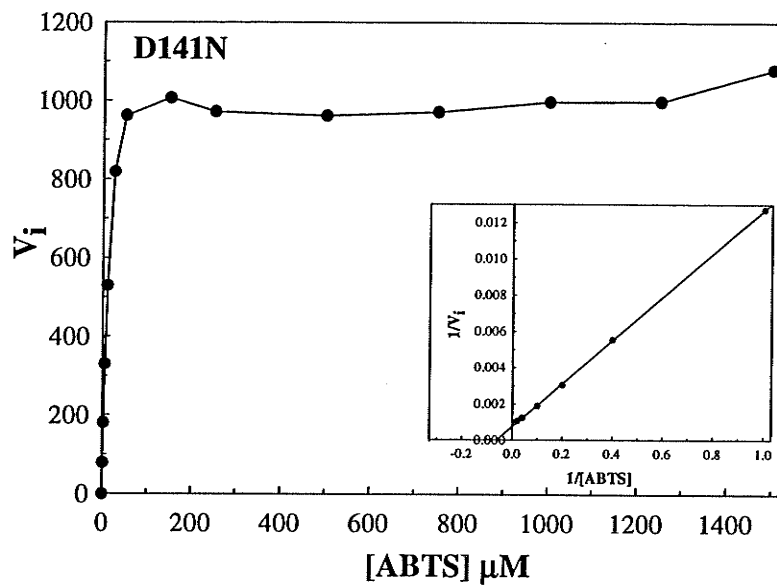


Figure 3.5. (continued)

**Table 3.6.** Comparison of the observed peroxidatic kinetic parameters of purified wildtype BpKatG and its variants, using ABTS as substrate.

Variant	$V_{\max}^a$	$K_m$ ( $\mu\text{M}$ )	$k_{\text{cat}}$ ( $\text{s}^{-1}$ )	$k_{\text{cat}}/K_m$ ( $\text{M}^{-1}\text{s}^{-1}$ )
Wt-BpKatG	$1,250 \pm 30$	$179 \pm 5$	$20.8 \pm 0.5$	$1.2 \times 10^5$
R108A	$435 \pm 24$	$185 \pm 2$	$7.3 \pm 0.4$	$3.9 \times 10^4$
R108K	$174 \pm 14$	$26 \pm 2$	$2.9 \pm 0.2$	$1.1 \times 10^5$
H112A	$4.6 \pm 0.1$	$4.7 \pm 0.2$	$0.08 \pm 0.002$	$1.6 \times 10^4$
H112N	$2.9 \pm 0.1$	$3.1 \pm 0.1$	$0.05 \pm 0.002$	$1.5 \times 10^4$
D141A	$556 \pm 2$	$13.2 \pm 1$	$9.3 \pm 0.03$	$7.0 \times 10^5$
D141N	$1,333 \pm 50$	$17.2 \pm 1$	$22.2 \pm 0.8$	$1.3 \times 10^6$
D141E	$833 \pm 20$	$62 \pm 2$	$13.9 \pm 0.33$	$2.2 \times 10^5$

<sup>a</sup>  $V_{\max}$  is expressed as  $\mu\text{moles of ABTS oxidized min}^{-1} \mu\text{mole heme}^{-1}$



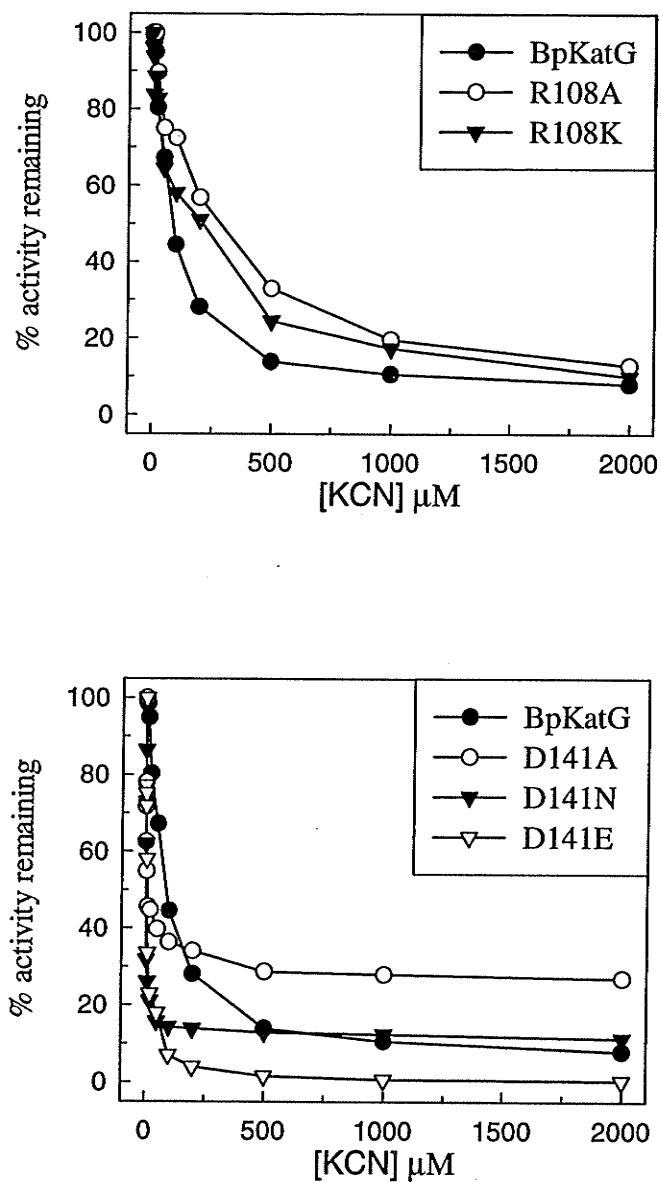


**Figure 3.6.** Comparison of the effect of potassium cyanide (KCN) on the catalase activity of wild type BpKatG and its variants.

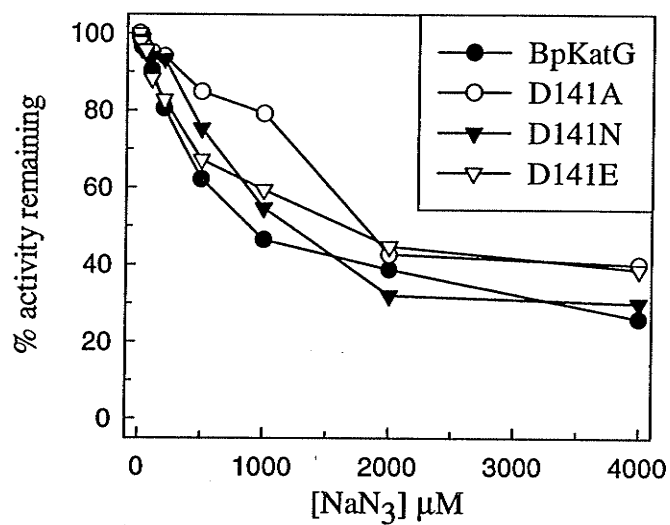
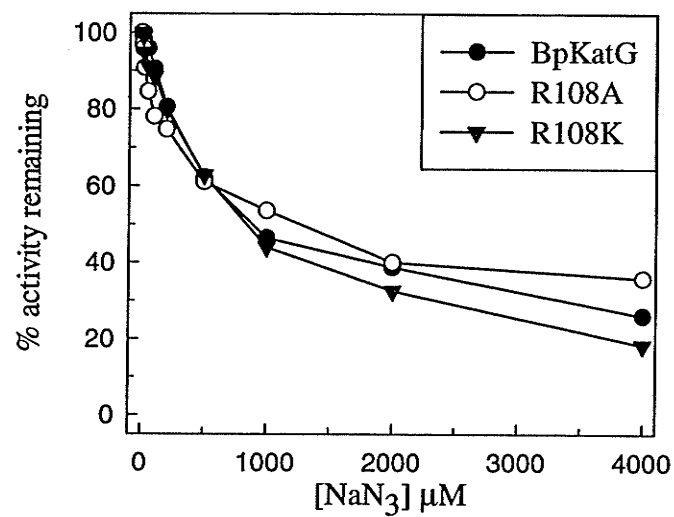


**Figure 3.7.** Comparison of the effect of sodium azide ( $\text{NaN}_3$ ) on the catalase activity of wild type BpKatG and its variants.

**Table 3.7.** Comparison of sensitivity of BpKatG and its variants to cyanide (KCN) or azide (NaN<sub>3</sub>).

Variant	[heme] <sup>a</sup>	[KCN] causing 50% inhibition ( $\mu$ M)	[NaN <sub>3</sub> ] causing 50% inhibition ( $\mu$ M)
Wt-BpKatG	3	88	890
R108A	9	285	1260
R108K	33	211	850
H112A		nd <sup>b</sup>	nd <sup>b</sup>
H112N		nd <sup>b</sup>	nd <sup>b</sup>
D141A	100	7.6	1800
D141N	26	3.2	1200
D141E	3	6.6	1650

<sup>a</sup> [protein] in reaction mixture expressed as : nM of heme.

<sup>b</sup> nd : not determined.

## 4. DISCUSSION

### 4.1. Structure-function studies on BpKatG

The apparent sequence similarity of catalase-peroxidases to members of the plant peroxidase family (about 20% identity), suggested that the active site residues would include arginine, tryptophan and histidine on the distal side of the heme based on analogy with the active site of yeast cytochrome *c* peroxidase (CCP) (Finzel *et al.*, 1984) and plant ascorbate peroxidase (APX) (Patterson *et al.*, 1995) identified in the crystal structures. This was confirmed in EcKatG (Hillar *et al.*, 2000) and SyKatG (Regelsberger *et al.*, 2000 and 2001), which revealed that changes to the identified residues caused both increases and decreases in activities. The equivalent active site residues in BpKatG include Arg108, His112 and Asp141 and modifications were introduced via site-directed mutagenesis to confirm their catalytic and structural roles, predicted by the crystal structures of HmCPx (Yamada *et al.*, 2001) and BpKatG (Carpena *et al.*, 2003). Trp111 of BpKatG is also in the active site but it has already been studied and reported by Donald *et al.* (2003).

The catalase and peroxidase activities of Arg108 variants were reduced 67% to 91% and 7% to 87%, respectively, compared to the wild type enzyme. The effect on peroxidase activity was dependent on the peroxidatic substrate used, presumably a size or structure effect, with o-dianisidine providing higher activity than ABTS. The properties of Arg108 variants are similar in most respects to the properties of Arg119 variants of SyKatG and Arg102 variants of EcKatG. The role of Arg108 is proposed to be the stabilization of compound I during its formation (Nicholls *et al.*, 2001), and any

modification of the residue, even to lysine, which removes the H-bonding interaction decreases the rate of compound I formation.

His112 variants of BpKatG exhibited less than 1% of wild type activity for catalase and peroxidase activities consistent with observations of His106 variants of EcKatG and His123 of SyKatG. Such a drastic effect on activity is consistent with the residue having a key role in initiating base catalysis to form compound I (Nicholls *et al.*, 2001).

The effect of changes in Asp141 depended on the replacing residue varying from a reduction of 90-98% in catalase activity for uncharged Ala or Asn to only a 13% reduction for Glu. In all cases there was little effect on peroxidase activity. Once again these results are similar to those for the Asp152 variants of SyKatG which exhibited significantly decreased catalase activity but increased peroxidase activity (Jakopitsch *et al.*, 2003). These results suggest that compound I formation is not affected by changes to Asp141 but that compound I reduction by  $\text{H}_2\text{O}_2$  requires a negatively charged side chain in this location. Jakopitsch *et al.* (2003) have proposed a mechanism in which the carboxylate of residue 141 (152 in SyKatG) is essential for binding  $\text{H}_2\text{O}_2$  along with Trp111 and facilitates proton removal (Figure 4.1). However based on an analogous situation in monofunctional catalases, an alternative or complementary role for Asp141 can be proposed. In EcHPH, Asp181 located in the main substrate access channel 12 Å from the heme and having a negatively charged residue at this location enhances the catalase reaction. The D181E variant exhibited normal catalase activity and contained an unbroken water matrix extending the full length of the substrate access channel, whereas the other variants, D181A, D181S and D181Q, were much less active and contained less water in the channel. It is proposed that an electrical potential field is created between the

negatively charged aspartate side chain at position 181 and the positively charged heme iron 12 Å distant was proposed, and that this field acts upon the electrical dipoles of water and H<sub>2</sub>O<sub>2</sub> forcing them into a common orientation. The oxygen atoms would be oriented towards the positively charged heme iron and hydrogen atoms oriented towards the negatively charged side chain of aspartate, thereby favouring hydrogen bond formation. In addition it provided an explanation for how H<sub>2</sub>O<sub>2</sub> would enter the active site in a preferred orientation as proposed by molecular dynamics studies (Chelikani *et al.*, 2003). The position of Asp141 of BpKatG is just 9 Å from the heme, slightly closer than Asp181 in HP11 making a similar mechanism a possibility. While the data from the Asp141 variant of BpKatG support such a hypothesis, it is not possible to distinguish between the electrical field mechanism and a direct ionic bond interaction as proposed by Jakopitsch *et al.* (2003). Indeed both mechanisms may be operative. Unfortunately, the X-ray diffraction data set is not at high enough resolution to accurately assign waters to the structure. Therefore, it is not possible to make any statement about water residency and a data set for an inactive variant such as D141A would be needed for comparison.

In conclusion, the data presented in this and the previous study of Trp111 (Donald *et al.*, 2003) have confirmed that the four active site residues of BpKatG, Arg108, His112, Trp111 and Asp141 all have differing roles in the catalytic mechanism. His112 and Arg108 are involved in compound I formation while Trp111 and Asp141 are involved in compound I reduction. This is described in Figure 4.1. The formation of catalase-peroxidase compound I proceeds from the resting state enzyme (1) through the introduction of H<sub>2</sub>O<sub>2</sub> (2) and its orientation in the active site by His and Arg (3). The O-O bond is broken and one molecule of H<sub>2</sub>O is released (4) to create compound I (5). The

reduction of compound I requires a second  $\text{H}_2\text{O}_2$  (6) which is oriented by Asp and Trp (7) leading to the formation of one molecule of  $\text{H}_2\text{O}$ , one molecule of  $\text{O}_2$  (8) and the native enzyme (1) (Nicholls et al., 2001).

#### 4.2. Future directions

The availability of the crystal structures of the catalase-peroxidases, BpKatG and HmCPx, has assisted researchers in the identification of residues involved in catalysis and structural roles. Unfortunately, only two variants, D141E and S324T, have so far been crystallized. This difficulty in obtaining crystals may be the result of incomplete formation of the covalent structure linking Trp111, Tyr238 and Met264 which disrupts the delicate crystal matrix. If optimum conditions could be found to assist the complete formation of the covalent structure, crystallization may ultimately be possible. The complexity of KatGs has recently been reinforced with the observation of an NADH oxidase activity (Singh *et al.*, 2004). In addition INH binds in the entrance channel near Ser324 and the hydrazine portion of INH is removed prior to combination with NAD to form the anti-tubercular drug, isonicotinoyl-NAD. Much work remains to be done to characterize these reactions and the substrate binding sites. For example, the structure of KatG presents several potential substrate-binding sites in its surface topography, one of which may be an NADH binding site and others for as yet unidentified substrates.

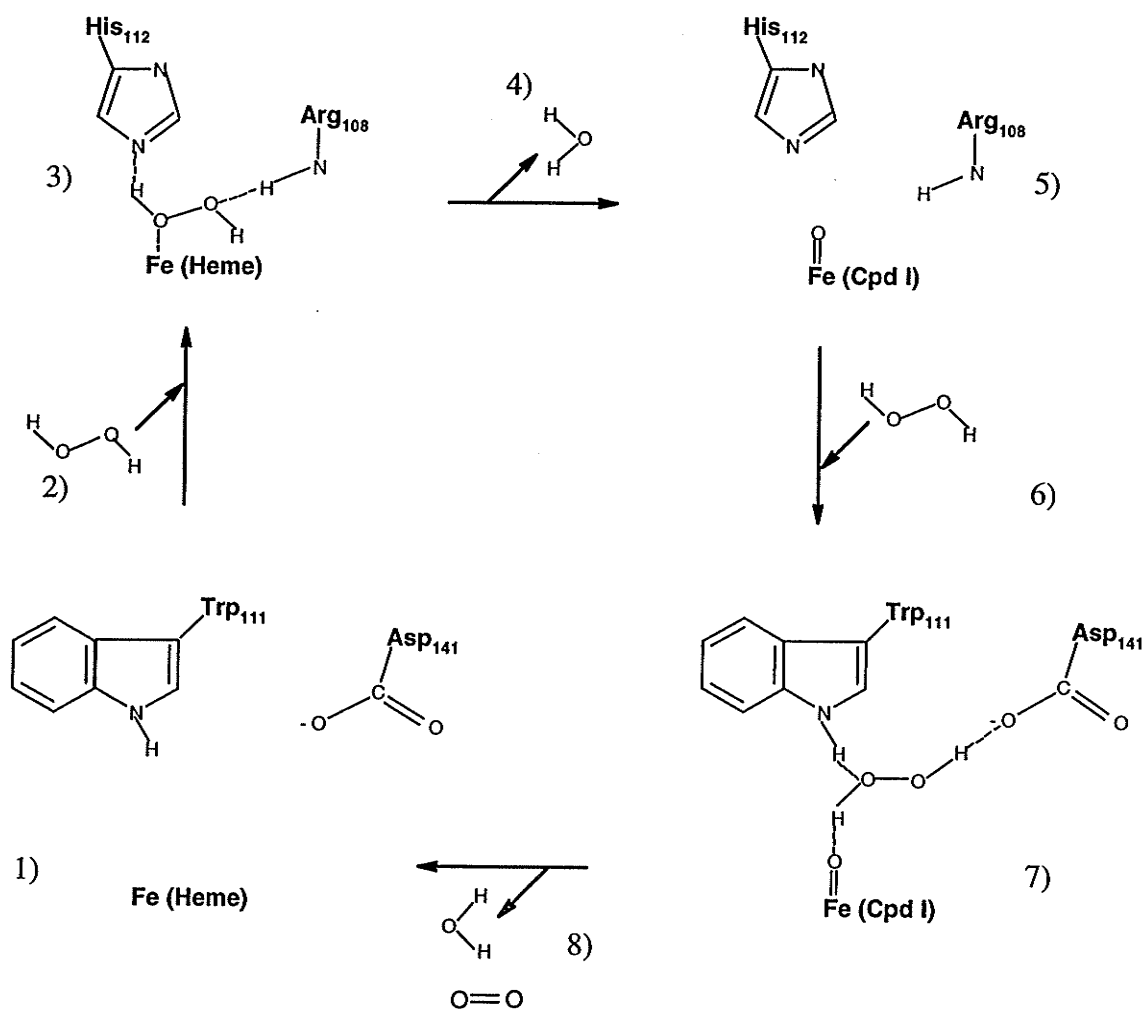


**Figure 4.1.** Hypothetical scheme for the mechanism of compound I formation and reduction during the catalytic turnover of catalase-peroxidase.



## 5. REFERENCES

- Ausubel, F. M., Brent, R., Kingston, R. E., Moore, D. D., Seidman, J. G., Smith, J. A., and Strunhl, K. (1989) *Current Protocols in Molecular Biology*. Green Publishing-Weiley Interscience. New York.
- Allgood, G. S., and Perry, J. J. (1986) Characterization of a manganese-containing catalase from the obligate thermophile *Thermoleophilum album*. *J. Bacteriol.* **168**: 563-567.
- Banerjee, A., Dubnau, E., Quemard, A., Balasubramanian, V., Um, K. S., Wilson, T., Collins, D., de Lisle, G., and Jacobs, W. R. Jr. (1994) InhA, a gene encoding a target for isoniazid and ethionamide in *Mycobacterium tuberculosis*. *Science*. **263**: 227-230.
- Berthet, S., Nykyri, L., Bravo, J., Maté, M. J., Berthet-Colominas, C., Alzari, P. M., Koller, F., and Fita, I. (1997) Crystallization and preliminary structural analysis of catalase-A from *Saccharomyces cerevisiae*. *Protein Sci.* **6**: 481-483.
- Bravo, J., Maté, M. J., Schneider, T., Switala, J., Wilson, K., Loewen, P. C., and Fita, I. (1999) Structure of catalase HPII from *Escherichia coli* at 1.9 Å resolution. *Proteins* **34**: 155-166.
- Bravo, J., Verdaguer, N., Tormo, J., Betzel, C., Switala, J., Loewen, P. C., and Fita, I. (1995) Crystal structure of catalase HPII from *Escherichia coli*. *Structure* **3**: 491-502.
- Cabiscol, E., Tamarit, J., and Ros, J. (2000a) Oxidative stress in bacteria and protein damage by reactive oxygen species. *Internatl. Microbiol.* **3**: 3-8.
- Cabiscol, E., Piulats, E., Echave, P., Herrero, E., and Ros, J. (2000b) Oxidative stress promotes specific protein damage in *Saccharomyces cerevisiae*. *J. Biol. Chem.* **275**: 27393-27398.
- Carpena, X., Guarné, A., Ferrer, J. C., Alzari, P. M., Fita, I., and Loewen, P. C. (2002) Crystallization and preliminary X-ray analysis of the hydroperoxidase I C-terminal domain from *Escherichia coli*. *Acta Crystallogr. D. Biol. Crystallogr.* **58**: 853-855.
- Carpena, X., Loprasert, S., Mongkolsuk, S., Switala, J., Loewen, P. C., and Fita, I. (2003) Catalase-peroxidase KatG of *Burkholderia pseudomallei* at 1.7 Å resolution. *J. Mol. Biol.* **327**: 475-489.
- Carpena, X., Perez, R., Ochoa, W. F., Verdaguer, N., Klotz, M. G., Switala, J., Melik-Adamyanyan, W., Fita, I., and Loewen, P. C. (2001) Crystallization and preliminary X-ray analysis of clade I catalases from *Pseudomonas syringae* and *Listeria seeligeri*. *Acta Crystallogr. D Biol. Crystallogr.* **57**: 1184-1186.

- Carpaena, X., Soriano, M., Klotz, M. G., Duckworth, H. W., Donald, L. J., Melik-Adamyan, W., Fita, I., and Loewen, P. C.** (2003) Structure of the clade I catalase, CatF of *Pseudomonas syringae*, at 1.8 Å resolution. *Proteins* **50**: 423-436.
- Carpaena, X., Switala, J., Loprasert, S., Mongkolsuk, S., Fita, I., and Loewen, P. C.** (2002) Crystallization and preliminary X-ray analysis of the catalase-peroxidase KatG from *Burkholderia pseudomallei*. *Acta Crystallogr. D. Biol. Crystallogr.* **58**: 2184-2186.
- Castro, L and Freeman, B. A.** (2001) Reactive oxygen species in human health and disease. *Nutrition*. **17**: 161-165.
- Chelikani, P., Fita, I., and Loewen, P. C.** (2004). Diversity of structures and properties among catalases. *Cell Mol Life Sci.* **61**: 192-208.
- Chelikani, P., Carpena, X., Fita, I., and Loewen, P. C.** (2003) An electrical potential in the access channel of catalases enhances catalysis. *J. Biol. Chem.* **278**: 31290-31296.
- Chung, C. T., Niemala, S. L., and Miller, R. H.** (1989) One-step preparation of competent *Escherichia coli*: transformation and storage of bacterial cells in the same solution. *Proc. Natl. Acad. Sci. U S A.* **86**: 2172-2175.
- Claiborne, A., and Fridovich, I.** (1979) Purification of the o-dianisidine peroxidase from *Escherichia coli* B. Physicochemical characterization and analysis of its dual catalatic and peroxidatic activities. *J. Biol. Chem.* **254**: 4245-4252.
- Demple, B. and Harrison, L.** (1994) Repair of oxidative damage to DNA: enzymology and biology. *Annu. Rev. Biochem.* **63**: 915-948.
- Dessen, A., Quemard, A., Blanchard, J. S., Jacobs, W. R. Jr., Sacchettini, J. C.,** (1995) Crystal structure and function of the isoniazid target of *Mycobacterium tuberculosis*. *Science.* **267**: 1638-1641.
- Donald, L. J., Krokhin, O. V., Duckworth, H. W., Wiseman, B., Deemagarn, T., Singh, R., Switala, J., Carpena, X., Fita, I., and Loewen, P. C.** (2003) Characterization of the catalase-peroxidase KatG from *Burkholderia pseudomallei* by mass spectrometry. *J. Biol. Chem.* **278**: 35687-35692.
- Espinal, M. A., and Raviglione, M. C.** (2003) Global epidemiology of tuberculosis. In *Tuberculosis*. (Madkour, M. M. ed) pp. 33-43. Springer-Verlag. Berlin Heidelberg.
- Finzel, B. C., Poulos, T. L., and Kraut, J.** (1984) Crystal structure of yeast cytochrome *c* peroxidase refined at 1.7 Å resolution. *J. Biol. Chem.* **259**: 13027-13036.
- Fita, I., and Rossmann, M. G.** (1985) The active center of catalase. *J. Mol. Biol.* **185**: 21-37.

- Fita, I., Silva, A. M., Murthy, M. R. N., and Rossmann, M. G.** (1986) The refined structure of beef liver catalase at 2.5 Å resolution. *Acta Crystallogr. B Biol. Crystallogr.* **42**: 497-515.
- Fraaije, M. W., Roubroeks, H. P., Hagen, W. R., and Van Berkel, W. J. H.** (1996) Purification and characterization of an intracellular catalase-peroxidase from *Penicillium simplicissimum*. *Eur. J. Biochem.* **235**: 192-198
- Fridovich, I.** (1977). Oxygen is toxic!. *BioScience.* **27**: 462-466.
- Fridovich, I.** (1978). The biology of oxygen radicals. *Science.* **201**: 875-880.
- Fridovich, I.** (1999). Fundamental aspects of reactive oxygen species, or what's the matter with oxygen? *Ann N Y Acad Sci.* **893**: 13-18.
- Gouet, P., Jouve, H. M., and Dideberg, O.** (1995) Crystal structure of *Proteus mirabilis* PR catalase with and without bound NADPH. *J. Mol. Biol.* **249**: 933-954.
- Heym, B., Alzari, P. M., Honore, N., Cole, S. T.** (1995) Missense mutations in the catalase-peroxidase gene, *katG*, are associated with isoniazid resistance in *Mycobacterium tuberculosis*. *Mol. Microbiol.* **15**: 235-245.
- Hidalgo, E., and Demple, B.** (1996) Adaptive responses to oxidative stress: The *soxRS* and *oxyR* Regulons. In *Regulation of gene Expression in Escherichia coli*. (Lin, E. C. C., and Lynch, A. S. eds) R. G. Landes Company.
- Hillar, A., Peters, B., Pauls, R., Loboda, A., Zhang, H., Mauk, A. G., and Loewen, P. C.** (2000) Modulation of the activities of catalase-peroxidase HPI of *Escherichia coli* by site-directed mutagenesis. *Biochemistry.* **39**: 5868-5875.
- Ho, R. Y. N., Liebman, J. F., and Valentine, J. S.** (1995) Biological reactions of dioxygen: an introduction. In *Active Oxygen in Biochemistry*, search series, Vol. 3, 1<sup>st</sup> edit., (Valentine, J. S., Foote, C. S., Greenberg, A., and Liebman, J. F., eds.) pp. 1-36, Blankie Academic and Professional, Glasgow.
- Imlay, J. A.** (2003) Pathway of oxidative damage. *Annu Rev Microbiol.* **57**: 395-418.
- Johnsson, K., King, D. S., and Schultz, P. G.** (1995) Studies on the mechanism of action of isoniazid and ethionamide in the chemotherapy of tuberculosis. *J. Am. Chem. Soc.* **117**: 5009-5010.
- Jakopitsch, C., Auer, M., Ivancich, A., Rüker, F., Furtmüller, P. G., and Obinger, C.** (2003) Total conversion of bifunctional catalase-peroxidase (KatG) to monofunctional peroxidase by exchange of a conserved distal side tyrosine. *J. Biol. Chem.* **278**: 20185-20191.

Jakopitsch, C., Auer, M., Regelsberger, G., Jantschko, W., Furtmuller, P. G., Ruker, F., and Obinger, C. (2003) Distal site aspartate is essential in the catalase activity of catalase-peroxidases. *Biochemistry*. **42**: 5292-5300.

Jones, A. L., Beveridge, T. J., and Woods, D. E. (1996) Intracellular survival of *Burkholderia pseudomallei*. *Infect Immun*. **64**: 782-790.

Ko, T.-P., Safo, M. K., Musayev, F. N., Di Salvo, M. L., Wang, C., Wu, S.-H., and Abraham, D. J. (1999) Structure of human erythrocyte catalase. *Acta Crystallogr. D Biol. Crystallogr*. **56**: 241-245.

Kono, Y., and Fridovich, I. (1983) Inhibition and reactivation of Mn-catalase : Implications for valence changes at the active site manganese. *J. Biol. Chem*. **258**:13646-13648.

Kremer, L., Dover, L.G., Morbidoni, H. R., Vilcheze, C., Maughan, W. N., Baulard, A., Tu, S. C., Honore, N., Deretic, V., Sacchettini, J. C., Locht. C., Jacobs, W. R. Jr., Besra, G. S., (2003) Inhibition of InhA activity, but not KasA activity, induces formation of a KasA-containing complex in mycobacteria. *J. Biol. Chem*. **278**: 20547-20554.

Kunkel, T. A., Roberts, J. D., and Zankour, R. A. (1987) Rapid and efficient site-directed mutagenesis without phenotypic selection. *Methods Enzymol*. **154**: 367-382.

Leclarasamee, A. (2004) Recent development in melioidosis. *Curr. Opin. Infect Dis*. **17**: 131-136.

Lei, B., Wei, C. J., and Tu, S. C. (2000) Action mechanism of antitubercular isoniazid. Activation by *Mycobacterium tuberculosis* KatG, isolation, and characterization of inhA inhibitor. *J Biol Chem*. **275**: 2520-2526.

Levy, E., Eyal, Z., and Hochman, A. (1992) Purification and characterization of a catalase-peroxidase from the fungus *Septoria tritici*. *Arch. Biochem.Biophys*. **296**: 321-327.

Loew, O. (1900) Physiological studies of Connecticut leaf tobacco. U.S. Dept. of Agri. Repts. **56**: 5-57.

Loewen, P. C. (1997) Bacterial Catalases. In *Oxidative Stress and the Molecular Biology of Antioxidant Defenses*. (Scandalios, J. G., ed) pp. 273-308. Cold Spring Harbor Press, Cold Spring Harbor, New York.

Loewen, P. C. (1999) Catalase. In *the Encyclopedia of Molecular Biology*. (Creighton, T. E. ed) pp. 351-353. Wiley J. and Sons, New York.

- Loewen, P.C., Carpena, X., Rovira, C., Ivancich, A., Perez-Luque, R., Haas, R., Odenbreit, S., Nicholls, P., and Fita, I. (2004) Structure of *Helicobacter pylori* catalase, with and without formic acid bound, at 1.6 Å resolution. *Biochemistry*. **43**:3089-3103.
- Loewen, P. C., Klotz, M. G., and Hassett, D. J. (2000) Catalase-an "Old" enzyme that continues to surprise us. *ASM News*. **66**: 76-82.
- Loewen, P. C., and Switala, J. (1986) Purification and characterization of catalase HP11 from *Escherichia coli* K12. *Biochem. Cell Biol.* **64**: 638-646.
- Loewen, P. C., Switala, J., Smolenski, M., and Triggs-Raine, B. L. (1990) Molecular characterization of three mutations in katG affecting the activity of hydroperoxidase I of *Escherichia coli*. *Biochem. Cell Biol.* **68**: 1073-1044.
- Loprasert, S., Sallabhan, R., Whangsuk, W., and Mongkolsuk, S. (2000) Characterization and mutagenesis of *fur* gene from *Burkholderia pseudomallei*. *Gene*. **254**: 129-137.
- Loprasert, S., Sallabhan, R., Whangsuk, W., and Mongkolsuk, S. (2002) The *Burkholderia pseudomallei oxyR* gene: expression analysis and mutant characterization. *Gene*. **296**: 161-169.
- Loprasert, S., Sallabhan, R., Whangsuk, W., and Mongkolsuk, S. (2003) Compensatory increase in *ahpC* gene expression and its role in protecting *Burkholderia pseudomallei* against reactive nitrogen intermediates. *Arch Microbiol.* **180**: 498-502.
- Loprasert, S., Whangsuk, W., Sallabhan, R., and Mongkolsuk, S. (2003) Regulation of the *katG-dpsA* operon and the importance of KatG in survival of *Burkholderia pseudomallei* exposed to oxidative stress. *FEBS Lett.* **542**: 17-21.
- Madkour, M. M., Al-Otaibi, K. E., and Swailem, R. A. (2003) Global epidemiology of tuberculosis. In *Tuberculosis*. (Madkour, M. M. ed) pp. 15-30. Springer-Verlag. Berlin Heidelberg.
- Maté, M. J., Zamocky, M., Nykyri, L. M., Herzog, C., Alzari, P. M., Betzel, C., Koller, F., and Fita, I. (1999) Structure of catalase-A from *Saccharomyces cerevisiae*. *J. Mol. Biol.* **286**: 135-139.
- Mdluli, K., Slayden, R. A., Zhu, Y., Ramaswamy, S., Pan, X., Mead, D., Crane, D. D., Musser, J. M., and Barry, C. E. 3<sup>rd</sup>. (1998) Inhibition of a *Mycobacterium tuberculosis* beta-ketoacyl ACP synthase by isoniazid. *Science*. **280**:1607-1610.
- Mead, D. A., Skorupa, E. S., and Kemper B. (1985) Single-stranded DNA SP6 promoter plasmids for engineering mutant RNAs and proteins: synthesis of a 'stretched' preproparathyroid hormone. *Nucl. Acids. Res.* **13**: 1103-1118.

- Messner, K. R., and Imlay, J. A. (2002) Mechanism of superoxide and hydrogen peroxide formation by fumarate reductase, succinate dehydrogenase, and aspartate oxidase. *J. Biol. Chem.* **277**: 42563-42571.
- Middlebrook, G. (1952) Sterilization of tubercle bacilli by isonicotinic acid hydrazide and the incidence of variants resistant to the drug in vitro. *Am Rev Tuberc.* **65**: 765-767.
- Middlebrook, G. (1954) Isoniazid-resistance and catalase activity of tubercle bacilli; a preliminary report. *Am Rev Tuberc.* **69**: 471-472.
- Miyagi, K., Kawakami, K., and Saito, A. (1997) Role of reactive nitrogen and oxygen intermediates in gamma interferon-stimulated murine macrophage bactericidal activity against *Burkholderia pseudomallei*. *Infect Immun.* **65**: 4108-4113.
- Morris, S., Bai, G. H., Suffys, P., Portillo-Gomez, L., Fairchok, M., and Rouse, D. (1995) Molecular mechanisms of multiple drug resistance in clinical isolates of *Mycobacterium tuberculosis*. *J. Infect. Dis.* **171**: 954-960.
- Murthy, M. R. N., Reid, T. J., Sicignano, A., Tanaka, N., and Rossmann, M. G. (1981) Structure of beef liver catalase. *J. Mol. Biol.* **152**: 465-499.
- Murshudov, G. N., Melik-Adamyan, W. R., Grebenko, A. I., Barynin, V. V., Vagin, A. A., Vainshtein, B. K., Dauter, Z., and Wilson, K. (1982) Three-dimensional structure of catalase from *Micrococcus lysodeikticus* at 1.5 Å resolution. *FEBS Lett.* **312**: 127-131.
- Nicholls, P., Fita, I., and Loewen, P. C. (2001) Enzymology and structure of catalases, *Adv. Inorg. Chem.* **51**: 51-106.
- Nguyen, N., Claparols, C., Bernadou, J., and Meunier, B. (2001) A fast and efficient metal-mediated oxidation of isoniazid and identification of isoniazid-NAD(H) adducts. *Chembiochem.* **2**: 877-883.
- Patterson, W. R., and Poulos, T. L. (1995) Crystal structure of recombinant pea cytosolic ascorbate peroxidase. *Biochemistry* **34**: 4331-4341.
- Putnam, C. D., Arvai, A. S., Bourne, Y., and Tainer, J. A. (1999) Active and inhibited human catalase structures: ligand and NADPH binding and catalytic mechanism, *J. Mol. Biol.* **296**: 295-309.
- Quemard, A., Lacave, C., and Laneelle, G. (1991) Isoniazid inhibition of mycolic acid synthesis by cell extracts of sensitive and resistant strains of *Mycobacterium aurum*. *Antimicrob. Agents. Chemother.* **35**: 1035-1039.

Regelsberger, G., Jakopitsch, C., Furtmuller, P. G., Rueker, F., Switala, J., Loewen, P. C., and Obinger, C. (2001) The role of distal tryptophan in the bifunctional activity of catalase-peroxidases. *Biochem. Soc. Trans.* **29**: 99-105.

Regelsberger, G., Jakopitsch, C., Ruker, F., Krois, D., Peschek, G. A., and Obinger, C. (2000) Effect of distal cavity mutations on the formation of compound I in catalase-peroxidases. *J. Biol. Chem.* **275**: 22854-22861

Rørth, M. and Jensen, P. K. (1967) Determination of catalase activity by means of the Clark oxygen electrode. *Biochim. Biophys. Acta.* **139**: 171-173.

Rozwarski, D. A., Grant, G. A., Barton, D. H., Jacobs, W. R. Jr., and Sacchettini, J. C. (1998) Modification of the NADH of the isoniazid target (InhA) from *Mycobacterium tuberculosis*. *Science.* **279**: 98-102.

Rouse, D. A., DeVito, J. A., Li, Z., Byer, H., and Morris, S. L. (1996) Site-directed mutagenesis of the katG gene of *Mycobacterium tuberculosis*: effects on catalase-peroxidase activities and isoniazid resistance. *Mol. Microbiol.* **22**:583-592.

Saint-Joanis, B., Souchon, H., Wilming, M., Johnsson, K., Alzari, P. M., and Cole, S. T. (1999) Use of site-directed mutagenesis to probe the structure, function and isoniazid activation of the catalase/peroxidase, KatG, from *Mycobacterium tuberculosis*. *Biochem. J.* **338**: 753-760.

Sambrook, J., Fritsch, E. F., and Maniatis, T. (1989) *Molecular Cloning : A Laboratory Manual*. Cold Spring Harbour Laboratory. Cold Spring Harbour Press. New York.

Sanger, F. S., Nicklen, S., and Coulson, A. R. (1977) DNA sequencing with chain-terminating inhibitors. *Proc. Natl. Acad. Sci. U S A.* **74**: 5463-5467.

Singh, R., Wiseman, B., Deemagarn, T., Donald, L., Duckworth, H., Carpena, X., Fita, I., and Loewen, P. C. (2004) Catalase-peroxidases (KatG) exhibit NADH oxidase activity. *J. Biol. Chem.* In press.

Smith, A. T., Santama, N., Dacey, S., Edwards, M., Bray, R. C., Thorneley, R. N., and Burke, J. F. (1990) Expression of a synthetic gene for horseradish peroxidase C in *Escherichia coli* and folding and activation of the recombinant enzyme with  $\text{Ca}^{2+}$  and heme. *J. Biol. Chem.* **265**: 13335 - 13343.

Storz, G., and Imlay, J. A. (1999) Oxidative stress. *Curr. Opin. Microbiol.* **2**: 188-194.

Takayama, K., Wang, L., and David, H. L. (1972) Effect of isoniazid on the in vivo mycolic acid synthesis, cell growth, and viability of *Mycobacterium tuberculosis*. *Antimicrob. Agents. Chemother.* **2**: 29-35.

- Takayama, K., Schnoes, H. K., Armstrong, E.L., and Boyle, R.W.** (1975) Site of inhibitory action of isoniazid in the synthesis of mycolic acids in *Mycobacterium tuberculosis*. *J. Lipid. Res.* **16**: 308-317.
- Triggs-Raine, B. L., Doble, B. W., Mulvey, M. R., Sorby, P. A., and Loewen, P. C.** (1988) Nucleotide sequence of *katG*, encoding catalase HPI of *Escherichia coli*. *J. Bacteriol.* **170**: 4415-4419.
- Vainshtein, B. K., Melik-Adamyany, W. R., Barynin, V. V., Vagin, A. A., and Grebenko, A. I.** (1981) Three-dimensional structure of the enzyme catalase. *Nature* **293**: 411-412.
- Vainshtein, B. K., Melik-Adamyany, W. R., Barynin, V. V., Vagin, A. A., Grebenko, A. I., Borisov, V. V., Bartels, K. S., Fita, I., and Rossmann, M. G.** (1986) Three-dimensional structure of catalase from *Penicillium vitale*, at 2.0 Å resolution. *J. Mol. Biol.* **188**: 49-61.
- Vieira, J. and Messing, J.** (1987) Production of single-stranded plasmid DNA. *Methods Enzymol.* **153**: 3-11.
- Von Ossowski, I., Mulvey, M. R., Leco, P. A., Borys, A., and Loewen, P. C.** (1991) Nucleotide sequence of *Escherichia coli katE*, which encodes catalase HPII. *J. Bacteriol.* **173**: 514-520.
- Wada, K., Tada, T., Nakamura, Y., Kinoshita, T., Tamoi, M., Shigeoka, S., and Nishimura, K.** (2002). Crystallization and preliminary X-ray diffraction studies of catalase-peroxidase from *Synechococcus* PCC 7942. *Acta Crystallogr D Biol Crystallogr.* **58**: 157-159.
- Waldo, G. S., Fronko, R. M., and Penner-Hahn, J. E.** (1991) Inactivation and reactivation of manganese catalase: oxidation-state assignments using X-ray absorption spectroscopy. *Biochemistry.* **30**: 10486-10490.
- Weber, K., Pringle, J.R., and Osborn, M.** (1972) Measurement of molecular weights by electrophoresis on SDS-polyacrymide gels. *Methods Enzymol.* **26**: 3-27.
- Welinder, K. G.** (1991) Bacterial catalase-peroxidases are gene duplicated members of the plant peroxidase superfamily. *Biochim Biophys Acta.* **1080**: 215-220.
- Wilming, M., and Johnsson, K.** (1999) Spontaneous formation of the bioactive form of the tuberculosis drug isoniazid. *Angew. Chem. Int. Ed.* **38**: 2588-2590.
- Winder, F. G., and Collins, P. B.** (1970) Inhibition by isoniazid of synthesis of mycolic acids in *Mycobacterium tuberculosis*. *J. Gen. Microbiol.* **63**: 41-48.
- Worthington Enzyme Catalog.** (1969) *Peroxidase (Hoseradish)*, p. 4-69. Worthington Biochemical Corp., Freehold, New Jersey.



**Yamada, Y., Fujiwara, T., Sato, T., Igarashi, N., and Tanaka, N.** (2002). The 2.0 Å crystal structure of catalase-peroxidase from *Haloarcula marismortui*. *Nat Struct Biol.* **9**: 691-695.

**Yamada, Y., Saijo, S., Sato, T., Igarashi, N., Usui, H., Fujiwara, T., and Tanaka, N.** (2001) Crystallization and preliminary X-ray analysis of catalase-peroxidase from the halophilic archaeon *Haloarcula marismortui*. *Acta Crystallogr D Biol Crystallogr.* **57**:1157-1158.

**Yanisch-Perron, C., Vieira, J., and Messing, J.** (1985) Improved M13 phage cloning vectors and host strains: nucleotide sequences of the M13mp18 and pUC19 vectors. *Gene.* **33**: 103-119.

**Zhang, Y., Garbe, T., and Young, D.** (1993) Transformation with *katG* restores isoniazid-sensitivity in *Mycobacterium tuberculosis* isolates resistant to a range of drug concentrations. *Mol. Microbiol.* **8**: 521-524.

**Zhang, Y., Heym, B., Allen, B., Young, D., and Cole, S.** (1992) The catalase-peroxidase gene and isoniazid resistance of *Mycobacterium tuberculosis*. *Nature.* **358**: 591-593.